



HAL
open science

Seasonal temporal dynamics of marine protists communities in tidally mixed coastal waters

Mariarita Caracciolo, Fabienne Rigaut-Jalabert, Sarah Romac, Frédéric Mahé, Samuel Forsans, Jean-Philippe Gac, Laure Arsenieff, Maxime Manno, Samuel Chaffron, Thierry Cariou, et al.

► To cite this version:

Mariarita Caracciolo, Fabienne Rigaut-Jalabert, Sarah Romac, Frédéric Mahé, Samuel Forsans, et al.. Seasonal temporal dynamics of marine protists communities in tidally mixed coastal waters. 2021. hal-03454364

HAL Id: hal-03454364

<https://hal.science/hal-03454364v1>

Preprint submitted on 29 Nov 2021

HAL is a multi-disciplinary open access archive for the deposit and dissemination of scientific research documents, whether they are published or not. The documents may come from teaching and research institutions in France or abroad, or from public or private research centers.

L'archive ouverte pluridisciplinaire **HAL**, est destinée au dépôt et à la diffusion de documents scientifiques de niveau recherche, publiés ou non, émanant des établissements d'enseignement et de recherche français ou étrangers, des laboratoires publics ou privés.

1 **Seasonal temporal dynamics of marine protists** 2 **communities in tidally mixed coastal waters**

3 Mariarita Caracciolo¹, Fabienne Rigaut-Jalabert², Sarah Romac¹, Frédéric Mahé³, Samuel
4 Forsans¹, Jean-Philippe Gac¹, Laure Arsenieff⁴, Maxime Manno¹, Samuel Chaffron^{5,6},
5 Thierry Cariou², Mark Hoebeke⁷, Yann Bozec¹, Eric Goberville⁸, Florence Le Gall¹, Loïc
6 Guilloux^{1,9}, Anne-Claire Baudoux¹, Colomban de Vargas^{1,5}, Fabrice Not¹, Eric
7 Thiébaud^{1,10}, Nicolas Henry^{1,5}, Nathalie Simon¹.

8 ¹Sorbonne Université, CNRS, Station Biologique de Roscoff, AD2M, UMR7144, Place
9 Georges Tessier, 29680 Roscoff, France.

10 ²Sorbonne Université, CNRS, Station Biologique de Roscoff, FR2424, 29680 Roscoff, France.

11 ³Cirad, UMR BGPI, F-34398, Montpellier, France.

12 ⁴Faculty of Biology, Technion – Israel Institute of Technology, Haifa 3200003, Israel

13 ⁵Research Federation for the study of Global Ocean Systems Ecology and Evolution,
14 FR2022/Tara Oceans GOSEE, 3 rue Michel-Ange, 75016 Paris, France.

15 ⁶Laboratoire des Sciences du Numérique de Nantes (LS2N), CNRS, UMR6004, Université de
16 Nantes, Ecole Centrale de Nantes, 44322 Nantes, France.

17 ⁷CNRS, Sorbonne Université, FR 2424, ABiMS Platform, Station Biologique de Roscoff,
18 29680 Roscoff, France

19 ⁸Unité biologie des organismes et écosystèmes aquatiques (BOREA), Muséum National
20 D'Histoire Naturelle, Sorbonne Université, Université de Caen Normandie, Université des
21 Antilles, CNRS, IRD, CP53, 61 rue Buffon 75005 Paris, France.

22 ⁹Mediterranean Institute of Oceanography (MIO), Campus de Luminy case 901, 163 Av. de
23 Luminy, 13288 Marseille cedex 9, France

24 ¹⁰Sorbonne Université, CNRS, OSU STAMAR, UMS2017, 4 Place Jussieu, 75252 Paris
25 cedex 05, France.

26

27 Corresponding authors :

28 #✉ : mariarita.caracciolo@sb-roscoff.fr, nathalie.simon@sb-roscoff.fr, [1](mailto:nicolas.henry@sb-</p></div><div data-bbox=)

29 roscoff.fr

30

31 Running title: Annually reoccurring marine protist communities in coastal waters

32

33 **Abstract**

34 Major seasonal community reorganizations and associated biomass variations are landmarks
35 of plankton ecology. However, the processes determining marine species and community
36 turnover rates have not been fully elucidated so far. Here, we analyse patterns of planktonic
37 protist community succession in temperate latitudes, based on quantitative taxonomic data
38 from both microscopy counts and ribosomal DNA metabarcoding from plankton samples
39 collected biweekly over 8 years (2009-2016) at the SOMLIT-Astan station (Roscoff, Western
40 English Channel). Considering the temporal structure of community dynamics (creating
41 temporal correlation), we elucidated the recurrent seasonal pattern of the dominant species
42 and OTUs (rDNA-derived taxa) that drive annual plankton successions. The use of
43 morphological and molecular analyses in combination allowed us to assess absolute species
44 abundance while improving taxonomic resolution, and revealed a greater diversity. Overall,
45 our results underpinned a protist community characterised by a seasonal structure, which is
46 supported by the dominant OTUs. We detected that some were partly benthic as a result of
47 the intense tidal mixing typical of the French coasts in the English Channel. While the
48 occurrence of these microorganisms is driven by the physical and biogeochemical conditions
49 of the environment, internal community processes, such as the complex network of biotic
50 interactions, also play a key role in shaping protist communities.

51 **Keywords**

52 Annual succession, Western English Channel, time-series data, marine protists, DNA
53 metabarcoding, temporal variability.

54

55 **1. Introduction**

56 Annual successions of species - and associated variations in biomass - are one of the
57 classical hallmarks of plankton ecology in both marine and freshwater systems (Cushing,
58 1959; Margalef, 1978; Sommer et al., 1986; Winder & Cloern, 2010; Sommer et al., 2012). In
59 temperate biomes, annual plankton biomass patterns classically involve some regularity in the
60 form of a phytoplankton spring bloom (Sverdrup, 1953; Cushing, 1959; Margalef, 1978) that
61 follows the increase of light availability in relation to a decrease in vertical mixing and
62 nutrient availability, and provides food to grazers. The resulting spring peak of zooplankton
63 leads to the decline of phytoplankton towards a mid-season biomass minimum while
64 subsequent food limitation and fish predation controls zooplankton biomass. The sequence of
65 planktonic taxa emerging along the course of this rhythmic phenomenon depends on regional
66 geographical, ecological and biogeochemical specificities (e.g., coastal *versus* shelf *versus*
67 oceanic conditions), but the overall annual reoccurrence of the same dominant species shows
68 striking regularities in a given habitat. Such annual persistent patterns of species successions
69 are well known for phytoplankton and zooplankton (Margalef, 1978; Modigh et al., 2001;
70 Ribera d'Alcalà et al., 2004). In most regions, these seasonal cycles linked to plankton
71 species phenologies have probably governed the evolution of life cycles and migratory

72 behaviors of organisms ranging from the smallest fishes to whales and birds (Cushing, 1969;
73 1990; Longhurst, 1998). Identifying these temporal patterns and determining their principal
74 environmental drivers are essential to reveal the mechanisms that drive species succession
75 and that shape community composition, and to predict how climate change is likely to modify
76 these patterns (Edwards & Richardson, 2003; Siano et al., 2021).

77 Predicting the consequences of environmental changes on the seasonal successions of
78 plankton species is extremely challenging since not all mechanisms that produce the sequence
79 of species along a seasonal cycle have been elucidated. Decades of research have emphasized
80 the major role of physical factors (e.g., light and turbulence; Margalef, 1978; Townsend et al.,
81 1992, 1994; Sommer et al., 2012; Barton et al., 2014) in pacing the annual oscillations of
82 plankton biomass and diversity. These factors, contingent to the annual climate cycle and
83 operating across various astronomic and geological time scales, would impose synchrony on
84 the dynamics of phytoplankton biomass (Smetacek, 1985; Sommer et al., 1986; Cloern, 1996)
85 in a similar way to terrestrial plants (Richardson et al., 2010; Craine et al. 2012). But seasonal
86 successions are also an emergent property of the community dynamics, where the complex
87 network of biotic interactions (e.g., predation, competition, parasitism, mutualism) and the
88 species internal clocks - that are tightly set by the photoperiod - determine the self-
89 organization and resilience of species assemblages for a specific time (Drake et al. 1990;
90 Dakos et al. 2009; Logares et al., 2018). Self-organization processes selected by
91 environmental filters, could be the major force shaping annual plankton successions. In other
92 words, intrinsic community biological factors, including interactions within and between
93 species and functional groups, could drive the stability of marine plankton through time. The

94 idea that biodiversity buffers ecosystem changes against environmental variations (Tilman,
95 1999; Tilman et al., 2006; Loreau & Manzancourt, 2013) matches results obtained from
96 manipulated microbiomes (Fernandez-Gonzalez et al., 2016) and theoretical studies (Dakos et
97 al., 2009). It could explain the strong temporal relationship that links species richness and
98 community-level properties (Cottingham et al., 2001; Loreau et al., 2001; Griffin et al.,
99 2009).

100 Characterized by particularly high dispersal capabilities, large population sizes, and
101 short generation time (Villarino et al., 2018), marine microorganisms represent about half of
102 overall carbon biomass and play key roles in global biogeochemical fluxes (Falkowski et al.
103 2008; Bar-On and Milo, 2019). They are responsible for nearly all of the primary production
104 and respiration occurring in the marine realm (Moran, 2015). While annual species
105 successions have been hard to demonstrate for microorganisms (i.e., viruses, bacteria, archaea
106 and protists; phototrophic and non-phototrophic microeukaryotes), especially for those with
107 sizes under 10 μm which are difficult to identify under a microscope, the use of High
108 Throughput Sequencing (HTS) and metagenomics approaches has shown that marine
109 microbial communities exhibit clear annual patterns of species or Operational Taxonomic
110 Units (OTU) successions (Fuhrman et al., 2006, 2015; Gilbert et al., 2012; Bunse & Pinhassi,
111 2017; Giner et al., 2018; Käse et al., 2020). Given the extraordinary roles of microscopic
112 plankton in ocean ecology, being able to document their dynamics in space and time is of
113 tremendous importance to predict future changes that will occur in the next decades.

114 Here, we report pluri-annual patterns of protists community dynamics at the Roscoff
115 SOMLIT-Astan station, a coastal long-term time-series sampling site located off the French

116 coast of the Western English Channel (WEC) (Fig. 1). The English Channel (EC) is an
117 epicontinental sea which stands as a biogeographical crossroad between the warm-temperate
118 Atlantic system and the cold-temperate North Sea and Baltic continental system of Northern
119 Europe. Significant biological shifts, including species replacements or major changes in
120 species abundances and distributions, have been documented in the English Channel since
121 over a century in response to climate change and other anthropogenic drivers (Boalch et al.,
122 1987; Southward et al., 2005; Mieszkowska et al., 2014). There are indications that current
123 anthropogenic climate changes have already impacted pelagic and benthic compartments and
124 affected the productivity of this shelf sea (see for example, Beaugrand et al., 2002; Genner et
125 al., 2004; Hiscock et al., 2004; Southward et al., 2005, Widdicombe et al. 2010). The EC is a
126 zone of high turbulence due to strong tidal currents. A seasonal thermocline, occurring from
127 May to October, is only reported in its western entrance, offshore and along the UK coasts
128 (Pingree and Griffiths, 1980). In these seasonally stratified waters sampled regularly by the
129 Plymouth L4 Western Channel Observatory (Pingree and Griffiths, 1978), plankton temporal
130 dynamics has been recently explored (Widdicombe et al., 2010; Edwards et al., 2013, Barton
131 et al., 2020) and both seasonal and inter-annual changes in abundance were observed along
132 with significant long-term changes in community composition and reorganization of plankton
133 food web (Molinero et al., 2013; Reygondeau et al., 2015). The temporal dynamics of
134 planktonic communities in the permanently well-mixed waters that characterize the French
135 coasts of the WEC have been less intensively studied. In this region, the hydrodynamics is
136 mostly driven by intense tidal currents and density gradients due to inflows of small rivers.
137 These features are at the origin of strong physical and biogeochemical heterogeneity and of a
138 mosaic of interconnected benthic and pelagic habitats (Dauvin et al., 2008; Delavenne et al.,

139 2013; Gac et al., 2020). At the Roscoff time series station, the daily and seasonal biological
140 cycles seem to maintain biogeochemical fluxes in steady state, for example in terms of CO₂
141 fluxes (Gac et al., 2020), suggesting that the complex plankton community has the capacity to
142 buffer environmental changes at the scale of at least a few years.

143 In this study, our aim was to (i) describe the seasonal dynamics of the protist
144 eukaryotic community in this macro tidal coastal marine plankton ecosystem across multiple
145 years, and (ii) explore how environmental factors interact with the dominant biotic
146 compartment at different time scales. We analysed time-series of phytoplankton cell
147 microscopy counts and DNA amplicons V4 sequence abundances generated from plankton
148 samples collected over a period of 8 years (2009-2016). We unveil the protist community
149 dynamics of this region in details, and provide new data on the dynamics of taxa that cannot
150 be studied with classical microscopic techniques. Our results suggest that the temporal
151 structure of environmental factors has an important influence on the seasonal dynamics of the
152 community that exhibited recurrent successions over the 8-year period. Self-organization
153 processes selected by environmental filters are suspected to be a major force shaping annual
154 plankton successions.

155

156 **2. Material and methods**

157 **2.1 Sampling station**

158 The SOMLIT-Astan sampling station is located in the western English Channel, 3.5
159 km off Roscoff (Brittany, France) (60 m depth, 48°46'18" N–3°58'6" W, Fig. 1). In this

160 coastal station, considered as representative of the French Western English Channel (Tréguer
161 et al., 2014) intense tidal mixing (tidal range up to 10 m) and winds prevent summer
162 stratification (Grall 1972, Martin-Jezequel 1983, Sournia et al. 1987). This station is also
163 under limited influence by coastal freshwater inputs as nutrients loading from the adjacent
164 rivers is rapidly diluted by tidal currents (L'Helguen et al. 1996, Wafar et al. 1983, Tréguer et
165 al. 2014), but it is strongly impacted by the weather conditions that can be rough in the area
166 with frequent gusts of wind and storms. Monitoring of the hydrology and phytoplankton at
167 the SOMLIT-Astan station has been implemented in 2000 (Guilloux et al. 2013), and is
168 currently operated in the frame of the SOMLIT (Service d'Observation en Milieu LITtoral,
169 since 2000, <http://somlit.epoc.u-bordeaux1.fr/>) and PHYTOBS (PHYtoplankton
170 OBServatory, since 2018) national monitoring programs. Plankton samples are collected bi-
171 monthly at the SOMLIT-Astan station during high neap tide at surface (1 m depth) using a 5L
172 Niskin bottle, as well as hydrological parameters measured during the same dates. For this
173 study, the data corresponding to the period 2009 to 2016 were analysed.

174 **2.2 Environmental data**

175 Meteorological data (rainfall height, wind speed and direction, global radiation) and
176 hydrological data (temperature, nutrient concentrations, chlorophyll-*a* biomass, particulate
177 organic carbon and nitrogen, and suspended matter) for the period 2009 to 2016 were
178 obtained from MétéoFrance (<https://meteofrance.com/>) and the SOMLIT program
179 (<https://www.somlit.fr/parametres-et-protocoles/>), respectively. Mean daily tidal amplitude
180 values were calculated from the water hourly heights available from the Service
181 Hydrographique et Océanographique de la Marine (SHOM, <https://data.shom.fr/>), and used as

182 a proxy of tidal mixing. Parameters related to light were obtained from the National
183 Aeronautic and Space Administration (NASA, <https://modis.gsfc.nasa.gov/data/dataproduct/>)
184 and the National Oceanic and Atmospheric Administration (NOAA,
185 <https://coastwatch.pfeg.noaa.gov/>). The average light received during the 8 days that
186 preceded each sampling dates was calculated from PAR (photosynthetically available
187 radiation, PAR8days, extracted from <https://modis.gsfc.nasa.gov/data/dataproduct/par.php>). The
188 diffuse attenuation coefficient for downwelling irradiance at 490 nm (Kd490), dependent on
189 the availability of ratios of remote sensing reflectance (Rrs) in the blue-green spectral region
190 (e.g., 490 - 565 nm) was also extracted (from
191 https://modis.gsfc.nasa.gov/data/dataproduct/kd_490.php). The North Atlantic Oscillation index
192 (NAO, Hurrell, 1995; Trigo et al., 2002) that influences the local meteorological conditions,
193 was obtained from NOAA (<https://www.ncdc.noaa.gov/teleconnections/nao/>). Protocols used
194 for the hydrological parameters by the SOMLIT are summarized below (Gac et al., 2020,
195 2021). Seawater temperature (T°C) was measured *in situ* using a Sea-bird SBE19+ CTD
196 profiler with an initial accuracy of +/- 0.005°C. Discrete salinity samples were measured on a
197 portasal salinometer with a precision of 0.002. Nutrient concentrations (NO₃⁻, NO₂⁻, PO₄³⁻
198 and SiO₄²⁻) were determined using an AA3 auto-analyser (Seal Analytical) following the
199 method of Aminot and K  rouel (2007) with an accuracy of 0.02 µmol L⁻¹, 1 nmol L⁻¹, 1 nmol
200 L⁻¹ and 0.01 µmol L⁻¹ for NO₃⁻, NO₂⁻, PO₄³⁻ and SiO₄²⁻, respectively. Ammonium (NH₄⁺)
201 concentrations were determined using the indophenol blue method of Koroleff (1969). To
202 determine chlorophyll-*a* concentrations (Chl-*a*), 0.5 L of seawater were filtered onto glass-
203 fibre filters (Whatman GF/F) and immediately frozen. Samples were extracted in 5 mL of
204 acetone, acidified with HCl and Chl-*a* concentrations, and were measured using a fluorometer

205 (model 10 analog fluorometer Turner Designs), according to EPA (1997), with an estimated
206 accuracy of $0.05 \mu\text{g L}^{-1}$. Protocols used to measure the biomass of particulate organic carbon
207 (POC), particulate organic nitrate (PON) and suspended matter (MES) are described in the
208 SOMLIT website.

209 **2.3 Phytoplankton microscopic counts**

210 Samples (250 mL) of natural seawater intended for the acquisition of microscopic
211 counts were preserved with acid Lugol's iodine (Sournia, 1978, Guilloux et al. 2013), stored
212 in the dark, and further processed between 15 days and up to 1 year after sampling. Lugol's
213 iodine was added either back in the lab 1.5 to 2h after sampling or onboard immediately after
214 sampling. Cell counts were obtained from sub-samples that were gently poured into 50 mL
215 composite settling chamber (HYDRO-BIOS, Kiel), according to the standard Utermöhl
216 settlement method (Sournia, 1978; Guilloux et al., 2013). For some winter samples with low
217 cell densities, 100 mL settlement chambers were used. Counts and identification of taxa were
218 performed under an inverted light microscope (Leica DMI 300) at 200x and 400x
219 magnification. References used for species identification included Tomas (1997), Throndsen
220 et al. (2007), Hartley et al. (1996), Kraberg et al. (2010), Hoppenrath et al. (2009), Horner
221 (2002) and the Plankton*Net Data Provider (<http://www.planktonnet.eu/>). Taxonomic
222 assignation was achieved to the highest taxonomic rank that we could be reached, at species
223 level when possible. Raw microscopic counts were regularly stored in a local MS-Access
224 database and uploaded in the RESOMAR PELAGOS (<http://abims.sb-roscoff.fr/pelagos/>)
225 national database. The morphological taxa contingency table was carefully examined to
226 detect inconsistencies (e.g., abrupt changes in cell counts over the time series), and taxa for

227 which identification was uncertain were grouped into broader taxonomic categories. For
228 example, *Fragilaria* and *Brockmaniella* or *Cylindrotheca closterium* and *Nitzschia*
229 *longissima* which are difficult to distinguished between each other, were considered in
230 association in the same group of microscopic counts. The final morphological dataset (DOI:
231 10.5281/zenodo.5033180) consisted of counts of 146 taxonomical entities (taxa larger than
232 10µm in size) across 185 dates from 2009 to 2016.

233 **2.4 Protists DNA metabarcodes**

234 For the generation of DNA metabarcoding data, natural seawater from the Niskin
235 bottle was transported to the laboratory in a 10L Nalgene bottle and a volume of 5L was
236 collected onto 3µm polycarbonate membranes (47mm, Whatman; with the exception of May
237 25th 2010, when the sample was collected onto a 0.22µm sterivex filter, PVDF, Millipore).
238 Filters were preserved in 1.5mL of lysis buffer (Sucrose 256g/L, Tris 50mM pH8, EDTA
239 40mM) and stored at -80°C until further processing. A total of 185 samples were collected
240 between 2009 and 2016.

241 **2.4.1 Plankton DNA extraction, PCR amplification, and metabarcode sequencing**

242 The DNA extraction and generation of metabarcodes were performed using the exact
243 same procedure for all samples. Samples were first incubated 45min at 37°C with 100µL
244 lysozyme (20mg/mL), and 1h at 56°C with 20µL proteinase K (20mg/mL) and 100 µL SDS
245 20%. Nucleic acids were then extracted using a phenol-chloroform method (Sambrook et al.
246 1989), and purified using silica membranes from the NucleoSpin® PlantII kit (Macherey-
247 Nagel, Hoerd, France). DNA was eluted with 100µL Tris-EDTA 1x pH8 buffer and
248 quantified using a Nanodrop ND-1000 spectrophotometer and a Qubit 2.0 Fluorometer

249 instrument with dsDNA HS (High Sensitivity) assay (ThermoFisher Scientific, Waltham,
250 MA). Total DNA extracts were then used as templates for PCR amplification of the V4
251 region of the 18S rDNA (~380 bp) using the primers TAREuk454FWD1 (5'-
252 CCAGCASCYGC GGTAATTCC-3', *S. cerevisiae* position 565-584) and TAREukREV3 (5'-
253 ACTTTCGTTCTTGATYRA-3', *S. cerevisiae* position 964-981) (Stoeck et al. 2010) that
254 target most eukaryotic groups. The forward primer was linked to a tag, and both primers were
255 adapted for Illumina sequencing. PCR reactions (25 µl) contained 1x Master Mix Phusion
256 High-Fidelity DNAPolymerase (Finnzymes), 0.35 µM of each primer, 3%
257 dimethylsulphoxide and 5 ng of DNA. Each DNA sample was amplified in triplicates. The
258 PCR program had an initial denaturation step at 98°C during 30 s, 10 cycles of denaturation
259 at 98°C, annealing at 53°C for 30 s and elongation at 72°C for 30 s, then 15 similar cycles but
260 with 48°C annealing temperature, and a final step at 72°C for 10 min. Polymerase chain
261 reaction triplicates were pooled, and purified and eluted (30 µl) with NucleoSpin Gel and
262 PCR Clean-Up kit (Macherey-Nagel, ref: 740770.50 and 740770.250), and quantified with
263 the Quant-It PicoGreen double stranded DNA Assay kit (ThermoFisher). About 1 µg of
264 pooled amplicons were sent to Fasteris (www.fasteris.com, Plan-les-Ouates, Switzerland) for
265 high throughput sequencing on a 2x250bp MiSeq Illumina. Sequences were obtained in five
266 separate runs. Overall, ~ 7million unique sequences were obtained for a total of 185 samples
267 collected over the 8 years (> 3µm).

268 **2.4.2 Reads quality filtering and clustering**

269 Generation of 18S V4 rDNA Operational Taxonomic Units (OTUs) from the raw
270 sequencing reads and their assembly into a contingency table was obtained according to the

271 following pipeline (<https://nicolashenry50.gitlab.io/swarm-pipeline-astan-18sv4>). The paired-
272 end fastq files were demultiplexed and PCR primers were trimmed using Cutadapt v2.8
273 (Martin, 2011). Reads shorter than 100 nucleotides or untrimmed were filtered out. Trimmed
274 paired-end reads were merged using the fastq mergepairs command from VSEARCH v2.9.1
275 (Rognes et al., 2016) with a minimum overlap of 10 base pairs. Merged reads longer than 200
276 nucleotides were retained and clustered into OTUs using Swarm v2.2.2 with $d = 1$ and the
277 *fastidious* option (Mahé et al., 2014, 2015). The most abundant sequence of each OTU is
278 defined as the representative sequence. OTUs with a representative sequence considered to be
279 chimeric by the uchime_denovo command from VSEARCH or with a quality per base below
280 0.0002 were filtered out. Samples with a low number of reads were re-sequenced, for these
281 cases, only the readset with the highest number of reads was kept. Finally, OTUs which
282 appeared in less than 2 samples or with less than 3 reads were discarded (de Vargas et al.,
283 2015).

284 **2.4.3 Taxonomic assignments**

285 The V4 region was extracted from the 18S rDNA reference sequences from PR2
286 v4.12 (Guillou et al., 2013) with Cutadapt, using the same primer pair as for the PCR
287 amplification (maximum error rate of 0.2 and minimum overlap of 2/3 the length of the
288 primer). The representative sequences of each OTU were compared to these V4 reference
289 sequences by pairwise global alignment (usearch_global VSEARCH's command). Each OTU
290 inherits the taxonomy of the best hit or the last common ancestor in case of ties. OTUs with a
291 score below 80% similarity were considered as unassigned (Mahé et al., 2017; Stoeck et al.,
292 2010). In this study, focusing on the ecology of protists, only OTUs assigned to protist

293 lineages (eukaryotes which are not Metazoa, Rhodophyta, Phaeophyceae, Ulvophyceae or
294 Streptophyta) were considered. The final dataset (filtered OTU table, available at
295 DOI:10.5281/zenodo.5032451) contained 185 samples with a total of ~12.7 million sequence
296 reads and 15,271 OTUs affiliated to protist taxa. Assignment of the dominant OTUs (e.g.,
297 based on abundance and occurrence) was checked and refined manually by BLASTing them
298 (<https://blast.ncbi.nlm.nih.gov/Blast.cgi>) against the SILVA reference database
299 (<https://www.arb-silva.de/>). The origin and assignments of the best blast sequences (most of
300 which were 100% similar to our sequences) and of the corresponding strains or isolates were
301 carefully examined before taking the final taxonomic assignment decision (Table S1).

302 **2.5 Statistical analyses**

303 A summary of all analyses performed for the metabarcoding dataset is illustrated in
304 Fig. S1 and detailed procedures are available in GitLab
305 (<https://gitlab.com/MariaritaCaracciolo/roscoff-astan-time-series>). The analyses performed on
306 the morphological dataset were similar except that absolute abundance (cell counts) were
307 used for all analyses (no rarefaction step prior to the calculation of species richness, Shannon
308 Diversity Index and Jaccard similarity).

309 **2.5.1 Alpha and Beta diversity**

310 Standard alpha diversity metrics (Shannon Diversity Index and species richness) and
311 beta diversity metrics (Jaccard similarity index and Bray-Curtis similarity index; Krebs,
312 1999; Legendre & Legendre, 1998) were calculated for both the morphological and
313 metabarcoding datasets in order to analyse temporal changes in the composition and structure
314 of the protist communities Random subsampling (rarefaction) was used for the

315 metabarcoding dataset prior to the calculation of alpha diversity metrics and for the
316 calculation of the Jaccard similarity index in order to account for differences in sequencing
317 depth (i.e. total number of reads generated for a sample). Hellinger transformed data
318 (Legendre & Gallagher, 2001) were used for the calculation of Bray-Curtis dissimilarities (d
319 $= 1 - S$, where d is dissimilarity and S is similarity between samples). The transformation is
320 necessary for metabarcoding data where only relative abundance is meaningful.

321 **2.5. Detecting the temporal structure of plankton protist community**

322 In order to detect the temporal structure of the communities, we used distance-based
323 Moran's eigenvector maps (dbMEM) (Legendre & Gauthier, 2014). This method has the
324 potential to detect temporal structures produced by the species assemblage itself (through
325 auto-assemblage processes or autogenetic succession that involve species interactions,
326 Connell and Slatyer, 1977; Reynolds, 1984; McCook et al., 1994) provided that all influential
327 variables have been included in the analysis (Legendre and Gauthier, 2014). The dbMEM
328 eigenfunctions were computed from a distance matrix of the time separating observations,
329 truncated at a threshold corresponding to the largest time interval (lag= 44 days) (Legendre &
330 Gauthier, 2014). A forward selection procedure implemented in the package `adespatial`
331 ("forward.sel" function; Dray et al., 2018) was used to identify significant dbMEM. Among
332 the generated positive and negative dbMEM eigenfunctions ($n=55$ and $n=129$, respectively),
333 only 52 positive dbMEM were retained for the metabarcoding dataset and 47 for the
334 morphological dataset and used as explanatory variables for a redundancy analysis (RDA;
335 Ter Braak, 1994). This analysis consists in a series of regressions performed on community
336 matrices, i.e., OTU read abundance ($n=15,271$) or species cell counts ($n=146$) data. Only

337 OTUs present in at least 10 out of the 185 total samples were retained and the data were
338 Hellinger-transformed in order to (i) avoid overweighting rare species and (ii) be able to use
339 Euclidean distances that allow to compute RDA (Legendre & Gallagher, 2001). Significant
340 linear trends were then removed by computing the residuals, and Anova-like tests (with 999
341 permutations; Legendre, Oksanen & Braak, 2013) were implemented on the RDA to assess
342 the significance of each constrained axis (p value < 0.05). To calculate the proportion of the
343 variance explained by the significant axes, the adjusted R^2 of the RDA result was used.
344 Variance partitioning analyses allowed to filter out the variations due to temporal structures,
345 or autocorrelation, which accommodate the use of statistical tests to further assess which
346 environmental variables can influence community dynamics and species composition. All
347 parameters were first tested for collinearity, then successively used in a forward selection to
348 identify those significant to be tested for the study. To interpret temporal variations, we
349 calculated Spearman's rank correlation coefficients between the environmental parameters
350 and the eigenvalues of the first three axes of the RDA.

351 All statistical analyses were performed using the R environment (R version 4.1.0, R
352 Development Core Team, 2011). The R package "vegan" (Oksanen et al., 2013) and
353 "data.table" (Dowle and Srinivasan, 2018) were used to analyse frequency count data,
354 diversity, and to compute variance partitioning. The dbMEM analyses were performed using
355 the packages "ade4" (Dray and Dufour, 2007), "adespatial" (Dray et al., 2018), "ape 5.0"
356 (Paradis & Schliep, 2019) and "spdep" (Bivand & Wong, 2018). All figures were made with
357 "ggplot2" (Wickham, 2009).

358

359 **3. Results**

360 **3.1 Seasonal ecosystem dynamics at the SOMLIT-Astan station**

361 At the SOMLIT-Astan time-series station (Fig. 1), as expected in temperate marine
362 waters, both the hydrological parameters and phytoplankton biomass displayed clear seasonal
363 patterns over the 8-year period (2009-2016, Fig. 2). In this tidally mixed environment, mean
364 monthly temperatures varied from 9.8 (in March) to 15.7°C (in August). Mean monthly
365 salinity ranged between 35.1 and 35.4 (from spring to autumn). Seasonal changes in
366 chlorophyll *a* (Chl-*a*) concentration were characterized by broad summer maxima (from June
367 to August) and large inter-annual variability (Fig. S2). From 2009 to 2016, mean monthly
368 values were recorded between 0.4 and 1.5 $\mu\text{g L}^{-1}$ (in December and July, respectively), and
369 seasonal variations were synchronous with PAR (5.3 to 48.1 $\text{E m}^{-2} \text{day}^{-1}$). Mean monthly
370 minima in the main macronutrient concentration (PO_4^{3-} , SiO_4^{2-} and NO_2^-) that sustain
371 phytoplankton production were recorded in summer, when phytoplankton biomass was high;
372 however, macronutrients were never completely depleted (Fig. 2). Annual oscillations of pH
373 were also recorded with minima in autumn. Although sampling occurred consistently during
374 high neap tides, a clear biannual rhythm was detected in the mean monthly tidal amplitudes,
375 which varied between 3.1 and 4.2 m with the highest mean values in late spring (May)
376 according to the yearly change in the obliquity of the Earth's Equator. From 2009 to 2016, all
377 parameters exhibited large inter-annual variations and no significant decadal trend was
378 detected (Fig. S2).

379 The protists community structure also showed clear seasonal patterns according to
380 changes in alpha and beta diversity calculated from our morphological (only phytoplankton >

381 10 μm) and metabarcoding (all protist 18S V4rDNA OTUs > 3 μm) datasets (Fig. 3):
382 minimal Shannon diversity was recorded in spring and summer, when Chl-*a* biomass was the
383 highest, and maximum values in winter (Fig. 3A, B). This seasonal pattern, which is related
384 to changes in the seasonal pattern of species dominance, was consistent among taxonomic
385 groups although variations were encountered in the exact timing of the monthly minima of
386 some of the phyla or classes distinguished using metabarcoding (Fig. S3). For groups such as
387 the Cercozoa, an opposite signal was recorded (Fig. S3), with relatively high (low) Shannon's
388 diversity in spring and summer (winter). Taxa such as the MOCH-4 (marine Ochrophytes
389 without cultured representatives), Perkinsea or Raphidophyceae were recorded almost
390 exclusively during winter (Fig. S3).

391 The variations in the Jaccard and Bray-Curtis dissimilarities - calculated based upon
392 the morphological and the metabarcoding datasets along temporal distances between samples
393 - not only confirmed the strong seasonality in the structure of the community, but also
394 suggested gradual replacements of taxa along the year and recurrence in the annual sequence
395 of taxa over 8 years (Fig. 3B, D). The rates of changes in these similarities also showed clear
396 temporal variations for both datasets and appeared to follow a biannual rhythm, with relative
397 minima (maxima) in February-March and October (in May-July and December-January)
398 (Fig. S4). A higher variability was recorded for the morphological dataset, with a decrease in
399 similarity over time.

400 **3.2 Overall composition of the protists assemblages in coastal mixed** 401 **environments**

402 Based on microscopy counts of plankton > 10 μm , diatoms were clearly the
403 dominating group all year round and over the study period (86.5% and 74.4% of all cell
404 counts and taxonomic entities distinguished, respectively Fig. 4A, C). Dinoflagellates
405 covered another 7.1 % of all cells enumerated and accounted for 15.7% of total taxa richness.
406 Ciliates and haptophytes (more precisely Oligotrichea and Prymnesiophyta) accounted for 2.4
407 and 2.1 % of all cell counts. The other groups such as Undetermined_sp., Raphidophyceae,
408 Dictyochophyceae, Euglenophyceae, Pyramimonadophyceae, Xanthophyceae,
409 Prasinophyceae, Undetermined_Chlorophyta, accounted each for 1% or less than 1% (Fig.
410 4A). Each of these groups accounted for < 3% of the total number of morphological entities
411 (Fig. 4C).

412 Our metabarcoding approaches based on total DNA extracts from plankton >3 μm
413 uncovered a much wider diversity spectrum. A first-order, low-resolution taxonomic
414 assignation of all OTUs revealed the prevalence of Dinophyceae and diatoms in terms of
415 reads numbers over the whole study period (29.6 and 22.1% of all reads, Fig. 4B, S5).
416 Cryptophyta, Chlorophyta and Haptophyta that are primarily photosynthetic phyla accounted
417 for 11.3%, 4.4% and 1.1% of all reads counts, while the heterotrophic Cercozoa, Syndiniales
418 and Ciliophora, made up 8.1%, 7.5% and 3.5% of all read counts, respectively (Fig. 4B). The
419 contributions of the other eukaryotes, including Picozoa, Sagenista, Pseudofungi, Opalozoa,
420 Choanoflagellida, and Telonemia, were lower (< 2% of total reads, Fig. 4B). In terms of OTU
421 richness, the picture was slightly different since Dinophyceae and cercozoans appeared as the
422 first and second most diverse groups (18.6 and 16.6% of all OTUs, Fig. 4D), followed by
423 diatoms, Syndiniales and Ciliophora (11.4, 10.3 and 5.8% of all OTUs). OTU richness from

424 Sagenista (bicoecea and labyrinthulids), Opalozoa, Haptophyta, Cryptophyta, Chlorophyta,
425 Apicomplexa, Choanoflagellida, Fungi and Telonemia ranged from 3.9% (Sagenista) to 2.1%
426 (Telonemia) of the total number of OTUs. Other less diverse taxa belonging to 53 classes
427 (e.g., Pseudofungi, Chrysophyceae, Picozoa, Dictyochophyceae, Bolidophyceae,
428 Centroheliozoa, Radiolaria; see Fig. 4B for the complete list of the 52 classes) accounted for
429 less than 2% of all OTUs (Fig. 4D).

430 Clear seasonal variations were encountered at phylum or class levels for absolute cell
431 abundances (Fig. S5A). The abundances of diatom cells (>10um) generally peaked in late
432 spring and summer, while dinoflagellates maximal abundances were observed in late
433 summer. Important inter-annual variations were recorded in both the timing and intensity of
434 the annual peaks, however. For the Prymnesiophyceae, the interannual variations were
435 especially high, with exceptional developments of Haptophytes (corresponding to
436 *Phaeocystis globosa* blooms) in spring 2012. Seasonal and inter-annual variations were also
437 observed when contributions to total DNA reads abundances were examined, with maximal
438 contributions of diatoms and Dinophyceae in spring and summer, respectively, and of
439 Cryptophyta and Chlorophyta in summer and autumn, respectively. The contribution of
440 Cercozoa and Syndiniales (and other primarily heterotrophic, parasitic or saprotrophic groups
441 such as the Ciliophora, Picozoa, Opalozoa and Sagenista) started to increase in early winter
442 and were high during the first months of the year (Fig. S5B).

443 **3.3 Annual successions of protists at high taxonomic resolution**

444 Given the clear annual recurrence of morphological and molecular taxa detected with
445 beta diversity analyses (Fig. 3), we dug into seasonal variations of the protist assemblages at

446 a finer taxonomic scale. First, to integrate the broadest taxonomic diversity including the
447 smallest taxa, we used the metabarcoding dataset to calculate mean monthly relative
448 abundances of all OTUs and select the 10 most abundant taxa for each month. This resulting
449 list of 32 OTUs, due to the same OTUs being dominant in several months, contributed to
450 51.5% of all reads over the study period (Fig. 5A), and included diatoms, Dinophyceae,
451 Cryptophyta, Cercozoa, Syndiniales, as well as a Chlorophyta, a Picozoa, a MAST and a
452 Fungi. Sequences of both photosynthetic armored (*Heterocapsa*) and heterotrophic naked
453 (e.g. *Warnowia* and *Gyrodinium*) dinoflagellates dominated the sequences pools all year
454 round. The nanoplanktonic Cryptophytes *Teleaulax amphioxeia* (= *Plagioselmis prolunga*),
455 *T. gracilis* and *T. acuta* (all described as photosynthetic) and the green picoplanktonic algae
456 *Ostreococcus lucimarinus* also appeared as dominant taxa. The sequences of several parasitic
457 taxa such as the cercozoan *Cryothecomonas*, the dinoflagellates *Haplozoon* and Syndiniales,
458 and the fungi *Parengyodontium* also showed high prevalence (Fig. 5A). Diatom OTUs
459 identified as dominating the protist communities were assigned to *Minidiscus comicus*,
460 *Minidiscus variabilis* and *Guinardia delicatula*, and to the genera *Thalassiosira* and
461 *Arcocellulus* or *Minutocellus*. Although rather consistent over the 8 years, the temporal
462 sequence showed important inter-annual variations (Fig. S6): for example, the relative
463 contribution of reads assigned to the parasitic *Cryothecomonas* sp. and *C. linearis* were
464 particularly prominent during the winters 2012 and 2013, and in July 2013 and 2015,
465 respectively (Fig.S6A). Reads assigned to *Picozoa judraskeda* appeared only in 2016.

466 A closer examination of the diatoms species dynamics was achieved by calculating
467 mean monthly relative abundances of diatoms OTUs or cells and selecting the 5 most

468 abundant taxa for each month in the microscopic and metabarcoding datasets (Fig. 5B, C).
469 The resulting pools of cells or reads selected accounted for >75% and 70% of all counts/reads
470 in these two datasets, respectively. In microscopic counts, autumn and winter assemblages
471 were clearly dominated by species or genera with benthic affinities such as *Paralia* sp. and
472 the pennate morphological combinations corresponding to *Fragilaria/Brockmaniella* and
473 *Cylindrotheca closterium* /*Nitzschia longissima* (Fig. 5B). These taxa were replaced, from
474 mid-winter to early spring, by colonial genera with pelagic affinities and in particular by
475 *Thalassiosira* spp. (with *Thalassiosira levanderi/minima* reaching mean abundances of ~534
476 cells.L⁻¹ [35.83% of counts] in April) and *Skeletonema* spp. followed by *Dactyliosolen*
477 *fragilissimus* all along spring. The dominant species in late spring and summer was
478 *Guinardia delicatula* with the highest mean monthly abundances recorded in May and July
479 (with ~530 cells.L⁻¹ for both months, 43% and 26.16% of diatoms counts, respectively). The
480 contribution of the genus *Chaetoceros* was significant from spring until early winter (with *C.*
481 *curvisetus/debilis/pseudocurvisetus* and *C. wighamii* showing relative high contributions in
482 July and in winter, respectively). This picture of the mean yearly sequence of diatoms
483 appeared rather resilient over the period 2009-2016, but inter-annual variations were
484 apparent, with exceptional blooms of *Skeletonema* in early spring in 2011, 2013 and 2014,
485 and *Chaetoceros socialis* in July 2014. The contribution of the benthic diatoms associated to
486 the genera *Entomoneis/Amphiprora/Amphora* was exceptionally high in 2011.

487 The analysis of the genetic dataset confirmed the prevalence of the genera
488 *Thalassiosira* and *Guinardia* during spring and summer and the relative higher contribution
489 of *Navicula* species in winter, but gave a different picture of the seasonal succession within

490 the diatoms since the metabarcoding approach allowed deciphering the annual sequence of a
491 pool of persistently dominant nanodiatom taxa, such as the genera *Minidiscus*, *Cyclotella*,
492 *Arcocellulus/Minutocellus* or the species *Thalassiosira minima* (Fig 5C). In winter, *Minidiscus*
493 *comicus* appeared as the dominant species while from April, and all along the summer and
494 autumn, the contribution of *Thalassiosira* spp., *Cyclotella* and *Arcocellulus/Minutocellus*
495 increased sequentially. While inter-annual variations were observed in the yearly sequence
496 and contribution of dominant OTUs when individual years were considered (Fig. S6), the
497 overall dominance of the smallest taxa was observed every year.

498 **3.4 Temporal structure of planktonic protist community and ecological** 499 **drivers**

500 The use of a dbMEM analysis to decompose the temporal patterns of the community
501 allowed us to detect and investigate the environmental and biological processes involved in
502 the control of protist assemblages' dynamics at different timescales (Fig. 6). The dbMEM
503 eigenfunctions were retained by forward selection (47 and 52 positive MEMs, according to
504 the morphological and metabarcoding datasets) and explained 48.9% of the species and
505 52.2% of the OTUs variability in community composition, respectively. As expected,
506 seasonality - expressed in the first 2 constrained axes of the RDA - explained most of the
507 observed temporal variability (RDA1: 19.8-17.8% and RDA2: 11.5% and 9.3%, for
508 morphological and metabarcoding datasets respectively; Fig. 6B, D). For both datasets, the
509 winter and summer assemblages on the one hand, and the autumn and spring assemblages on
510 the other, were clearly distinguished on axes 1 and 2. Spring assemblages showed more
511 interannual variability, especially when the morphological dataset was considered (Fig. 6A).
512 The annual cycle was better delineated when the metabarcoding dataset was considered (Fig.

513 6C). For both datasets, the taxa/OTUs with the highest RDA1 and RDA2 scores
514 corresponded to dominating species (section 3.3 and Fig. 5) and displayed clear seasonal
515 variations in terms of cells or reads abundances (See Table 1 and Fig. 7A, B). For the
516 morphological datasets, the pelagic chain forming *Guinardia delicatula* and *Thalassiosira*
517 *levanderi/minima* and the benthic or tythropelagic taxa *Fragilaria/Brockmanniella*, *Paralia*
518 *sulcata* and *Psammodictyon pandutiforme* had the highest scores for RDA1 and/or RDA1.
519 For the metabarcoding dataset, the OTUs with the highest RDA1 and 2 scores also included
520 *G. delicatula*, but pointed as well to nanoplanktonic diatoms (such as *Minidiscus comicus*),
521 and to species belonging to other phyla or classes such as the Dinophyceae and Cercozoa, all
522 displaying strong seasonality (Fig. 7B and Table 1).

523 The axis 3 of the RDA (4.8 and 3.9 % of the variance explained for the morphological
524 and metabarcoding datasets respectively, Fig. 6B, D) expressed broad scale oscillations and a
525 persistent biannual rhythm in the protist community dynamics. In the morphological dataset,
526 *Skeletonema* sp. contributed most to axis 3 of the RDA. *G. delicatula* and *Chaetoceros*
527 *wighamii* also showed high contribution. In the metabarcoding dataset, the winter diatom *M.*
528 *comicus* and the Cercozoan *Cryothecomonas*, that exhibit a parasitic life styles, had the
529 highest contribution to this axis. Our analyses showed that some of the OTUs were not
530 detectable every year, suggesting an influence of the environment on the temporal patterns of
531 some protists.

532 To investigate the environmental factors that primarily drive seasonal protist
533 assemblages, we calculated Spearman rank correlation coefficients between the potential
534 explanatory variables and the first 3 axes of the RDA (Fig. 8A, B). Here, we considered the

535 environmental variables selected by forward selection for both datasets, namely: temperature,
536 phosphates (PO_4^{3-}), silicates (SiO_4^-), ammonia (NH_4^+), Chl-*a*, salinity, Suspended Matter
537 (MES) and the North Atlantic Oscillation (NAO) Index. Oxygen was selected only for
538 microscopy, and PAR, nitrate (NO_2^-), pH, and Delta N15 for metabarcoding. The analyses
539 suggested that macronutrients (PO_4^{3-} , NH_4^+ and to a less extent SiO_4^-), together with
540 temperature, PAR, and Chlorophyll-*a* showed the highest correlations with RDA1.
541 Temperature, salinity, oxygen, pH and NO_2^- showed the highest correlations with RDA2 (Fig.
542 8A, B). Even though environmental variables alone only accounted for 5% of the variance, a
543 large part of the variations in the community was explained by the temporal structure of the
544 environmental factors (26% and 24% for both datasets, respectively, Fig. 8C, D). The
545 temporal organization of the community explained most of the variations when considered
546 together with the environment (47% and 49%). These results suggest that the temporal
547 structures of the environmental factors are important drivers of the annual succession of
548 species, along with intrinsic community effects such as species interactions, reproductive
549 dynamics, and stochastic events not considered here.

550

551 **4. Discussion**

552 **4.1 Predictable cyclicality of protists successions in coastal pelagic habitats**

553 Annual successions of planktonic protists, in particular phytoplankton, have been
554 observed by early planktonologists (for diatoms and dinoflagellates, see for example Allen,
555 1936; Gran and Braarud, 1935) and have inspired the founding theories of ecological

556 successions (Margalef, 1963; Margalef et al., 1958, 1978). Recent temporal analyses of DNA
557 metabarcoding datasets from a wide range of biogeographical regions have confirmed that
558 such patterns are a general common feature of marine microbes, including prokaryotes and all
559 protists (Marquardt et al., 2016; Egge et al., 2015; Piredda et al., 2017). Some also noted the
560 overall stability of the yearly reoccurring sequences of taxa at the decade scale (see Fuhrman
561 et al., 2015 for bacteria and Lambert et al., 2019 or Giner et al., 2019 for protists).

562 Using morphological and DNA metabarcoding approaches, we clearly identified
563 annual succession patterns of taxa in the Western English Channel over the period 2009-
564 2016. The cyclic pattern was more distinct using metabarcodes (see Fig. 6A *versus* 6C),
565 however: by including some of the smallest eukaryotes, a greater diversity was therefore
566 assessed. Compared to microscopic counts (146 morphological taxa of mainly
567 microphytoplankton groups), genetic sequences data enabled to reach a much finer taxonomic
568 resolution (15,271 OTUs belonging to 53 different phyla and classes) and gave access to the
569 dynamics of nano-planktonic taxa (including some pico-) that are dominant at our site. For
570 example, the pico-planktonic green algae *Ostreococcus lucimarinus*, *Bathycoccus prasinos*
571 and *Micromonas* spp. or the nanoplanktonic diatoms *Minidiscus variabilis* and *M. comicus*,
572 are known major players of the microbial communities in the Western English Channel (Not
573 et al., 2004; Foulon et al., 2008; Arsenieff et al., 2020). DNA metabarcoding could also
574 capture the dynamics of naked dinoflagellates taxa (*Gyrodinium* and *Gymnodinium* species)
575 and heterotrophic, parasitic or endosymbiotic microeukaryotes such as the MAST,
576 *Cryothecomonas*, and Syndiniales species. Taxa such as *Cryothecomonas* that infects diatoms
577 and especially the genus *Guinardia* (Drebes et al., 1996; Peacock et al., 2014), and the

578 Syndiniales that parasite dinoflagellates (Chambouvet et al., 2008) are involved in the control
579 of phytoplankton blooms and thus in the overall stability of the system. These taxa, which
580 cannot be easily monitored using microscopy, are prominent all year round in terms of DNA
581 read abundances, and contributed significantly to the seasonal temporal variations captured
582 by the two first axes of our RDA analyses. Marine benthic protists indeed show high and
583 distinctively different diversity compared to planktonic species (Patterson et al., 1989),
584 especially in the Cercozoa (Forster et al., 2016), one of the dominant phyla at SOMLIT-
585 Astan.

586 Such regularities and stability in community composition over 8 years in the surface
587 waters of this megatidal region could be related to different factors. By transporting
588 planktonic species from and to adjacent habitats, tidal currents are known to increase
589 plankton dispersal, which is an important process in structuring communities (Vellend et al.,
590 2010). Therefore, tidal amplitude is intensifying the exchanges between communities
591 associated to the diverse habitats of the Morlaix Bay (Cabioch et al., 1968; Dauvin et al.,
592 2008; Gac et al., 2020). In habitats influenced by tidal mixing, high contributions of benthic
593 protists to the water column communities are classically observed (Hernandez-Farinas et al.,
594 2017); this phenomenon is amplified in winter, when pelagic species are less abundant and
595 winds increase vertical mixing (Mann & Lazier, 1991). Nevertheless, the induced high rates
596 of emigration and immigration do not apparently disrupt the seasonal oscillations in diversity
597 that was captured by the first 2 axes of our RDA analyses (Fig.6). By increasing the overall
598 diversity and by enhancing benthic-pelagic coupling (and potentially the interactions between
599 species), these forces may favor the overall stability of the system (Cardinale et al., 2012).

600 Our dbMEM analyses allowed us to uncover a clear and persistent biannual rhythm (axis 3 of
601 our RDA) in the protist community dynamics. This biannual pattern was also observed in the
602 monthly turnover rates of species over the 8 years (Fig. S4). However, no clear relationship
603 was found with annual variation in tidal amplitude which was not among the environmental
604 factors selected for correlation analyses (Fig.8).

605 We found a strong correlation between the first two axes of the RDA and temperature,
606 macronutrients and light (Fig. 8), suggesting that physical factors related to the annual
607 climate cycle are imposing synchrony to the protist seasonal dynamics (Cloern, 1996;
608 Sommer et al., 2012). Nevertheless, our results showed a more holistic vision, where most
609 part of the community dynamics was explained by the temporal structure of both
610 environmental and intrinsic factors (Fig. 8B and D).

611 **4.2 The annual sequence of dominant protists in temperate tidally-mixed habitats**

612 With observations conducted over 8 years using both microscopy and DNA
613 metabarcoding, our study improves our knowledge of pelagic protists in a tidally-mixed
614 coastal environment. In terms of phytoplankton, our study confirmed the importance of
615 diatoms (by far the most numerous taxa >10 μ m enumerated under microscopy),
616 dinoflagellates and green algae, but also highlighted the importance of Cryptophyta. The
617 DNA metabarcoding analysis provided new data about the seasonal sequence of important
618 heterotrophic dinoflagellates (i.e., Dinophyceae and Syndiniales) harboring diverse trophic
619 modes, and that of parasitic Cercozoa. Along the years 2009-2016, the prominence of the
620 chain-forming species *Guinardia delicatula* during spring and summer was confirmed by
621 both the morphological and metabarcoding datasets. This species is emblematic of the spring

622 and summer diatoms bloom in the Roscoff area (Grall, 1972; Martin-Jezequel, 1992; Sournia
623 et al., 1995; Guilloux et al., 2013; Arsenieff et al., 2019). It is one of the most recognized
624 species of planktonic communities in the English Channel and North Sea (Widdicombe et al.
625 2010; Caracciolo et al., 2021) and appear to be particularly successful in temperate tidally-
626 mixed habitats (Gomez and Souissi, 2007; Wiltshire et al., 2008; Peacock et al., 2012;
627 Schlüter et al., 2012; Hernandez-Farinas et al., 2014). Our analyses also tracked the classical
628 annually repeated sequence of diatoms that involves the development of microplanktonic
629 pelagic chain-forming species in spring (typically *Thalassiosira* spp., *G. delicatula*,
630 *Chaetoceros* spp.), as well as benthic and tychopelagic species in winter (e.g. *Paralia* sp. and
631 *Navicula* spp.). An annual sequence of nanodiatoms (involving species of the genera
632 *Minidiscus*, *Thalassiosira* and *Arcocellulus* / *Minutocellus*) was specifically revealed by the
633 metabarcoding approach. The prevalence of nanodiatoms, and especially of *Minidiscus* spp.
634 at the SOMLIT-Astan station has actually been confirmed by cultural approaches from the
635 SOMLIT-Astan station (Arsenieff et al., 2020). Nanodiatoms are have been identified as
636 prominent members of diatoms assemblages in other marine systems when adequate
637 detection techniques (cultural approaches, electron microscopy or HTS) were implemented
638 (Leblanc et al. 2018; Ribera l'Alcalà et al. 2004; Percopo et al. 2011).

639 If microphytoplanktonic dinoflagellates are usually present at relatively low
640 abundances in species microscopic counts in tidally-mixed waters off Roscoff (Sournia et al.,
641 1987; Guilloux et al., 2013), the contribution of dinoflagellates reads in the molecular dataset
642 was high all year round according to this study. Sequences corresponding to the dominant
643 reads were mostly assigned to nanoplanktonic species or naked species. Two OTUs assigned

644 to the genus *Heterocapsa* including the thecate species *H. rotundata* dominated read counts
645 for the whole period. This ubiquitous mixotrophic dinoflagellate, that has the potential to
646 switch from phototrophy to partial heterotrophy (Millette et al., 2017), may be favored at our
647 tidally-mixed coastal site, especially in August when light starts decreasing. Interestingly, *H.*
648 *rotundata* was also identified as a dominant taxon in the adjacent Penzé estuary (Chambouvet
649 et al., 2008), and as most abundant in recent microscopic counts obtained from our time-
650 series station where nanoplanktonic dinoflagellates were targeted (data not shown). Some
651 other dominant dinoflagellate OTUs detected in our metabarcoding dataset are either
652 heterotrophic or potentially mixotrophic (*Gyrodinium*, *Gymnodinium*, *Azadinium*, *Warnovia*
653 etc.), and some of them are purely parasitic (Syndiniales). The naked dinoflagellates
654 *Gyrodinium* and *Gymnodinium* spp. were also identified as prominent members of the
655 phytoplankton community in the stratified waters of the WEC, off Plymouth (Widdicombe et
656 al., 2010) and showed an increasing trend in abundance after 2001 (Hernández-Fariñas et al.,
657 2014). These dinoflagellates, that seem to thrive all year round, may be key predators for
658 diatoms. The increasing trend in average abundance of some dinoflagellates and the decrease
659 in diatoms has been recently documented in the Central North Atlantic Ocean and in the
660 North Sea (Leterme et al., 2005; Zhai et al., 2013), as well as in the English Channel
661 (Widdicombe et al., 2010).

662 Cryptophyta are important members of protists communities in coastal waters. Their
663 prominence in different regions of the ocean has been revealed using microscopy (Jochem,
664 1990), but also via flow cytometry, since the phototrophic members of this group can be
665 distinguished based on its phycoerythrin fluorescence (Dickie, 2001). Recent DNA

666 metabarcoding analyses have also revealed their prominence in coastal waters at Helgoland
667 Roads, North Sea (Käse et al., 2020). At the SOMLIT-Astan station, sequences identical to
668 different species of the genus *Teleaulax* were abundant in read counts. The highest proportion
669 of Cryptophyta reads were assigned to *Plagioselmis prolunga* (= *Teleaulax amphioxeia*), a
670 phototrophic species with a benthic-pelagic life-cycle (Altenburger et al., 2020) involved in
671 complex symbioses with the ciliate *Mesodinium rubrum* (Qiu et al., 2016). Besides, the later
672 species has an interesting behavior consisting of periodic dispersion away from the strong
673 superficial tidal currents, thus minimizing flushing losses (Crawford and Purdie, 1992).

674 We are aware that the description of the typical seasonal sequence of protists species
675 provided herein is still incomplete. Both microscopy and metabarcoding can provide biased
676 data, since the former does not consider the smallest taxa while the later can overestimate or
677 underestimate the proportions of taxa for which DNA is more easily extracted and amplified
678 (Santi et al. 2021). For example, the contribution of dinoflagellate to sequences reads
679 obtained from natural samples is a commonly reported bias due to the very high number of
680 18S copies in dinoflagellates (Gong and Marchetti, 2019). In our study, the contribution of
681 Haptophyta was probably underestimated since most species in this group are nano- or
682 picoplanktonic and were thus not reported in our morphological dataset, as the primers used
683 do not perfectly match with sequences of this group (McNichol et al., 2021). However, the
684 two datasets we used are complementary and allowed us to add important information about
685 the dynamics of dominant protists thriving in permanently mixed waters of the Western
686 English Channel. A deeper analysis of species dynamics in the different phyla for the
687 metabarcoding dataset will certainly provide more information in the future, especially since

688 reference sequences databases and taxonomic frameworks (required for accurate assignments
689 to genus or species levels) are constantly being updated and curated (Guillou et al., 2013;
690 Berney et al., 2017; Glöckner et al., 2017; del Campo et al., 2018).

691 **4.3 Environmental *versus* community intrinsic drivers of protistan plankton seasonal** 692 **dynamics**

693 Plankton phenology and seasonal species successions are periodic processes that are
694 tightly phased to astronomical forcing and associated annual cycles of temperature, solar
695 radiation, atmospheric heat input and photoperiod (Sverdrup, 1953; Cushing, 1959, Winder &
696 Cloern, 2010). While being structured by local physical and chemical conditions and
697 biological self-organization process, microbial eukaryotic communities, as a feed-back,
698 strongly impact biogeochemical cycles (Arrigo, 2005; Falkowski et al., 2008; Fuhrman,
699 2009). Spearman correlation coefficients calculated between environmental variables and the
700 first three axes of the RDA, confirmed a strong phasing between seasonal variations of
701 environmental parameters and protists assemblages. According to our analyses, the resilient
702 seasonal pattern in community dynamics is tightly linked to the temporal structure of
703 Photosynthetically Active Radiation, temperature, salinity and macronutrients (PO_4^3 , SiO_4^{2-} ,
704 NH_4^+ , Fig. 8A, and in a less extent NO_2^- , Fig. 8B). Thus, we identified the earth tilt and
705 rotation rhythms determining light intensity as the primary driver of the observed plankton
706 dynamics, in association with cyclical variations in water temperature and principal
707 macronutrients concentration. Those factors are more important with respect to local
708 hydrodynamic conditions, nevertheless, local factors such as salinity and pH showed high
709 correlation with the second axes (Fig. 8B), suggesting that phytoplankton variability also

710 depends on additional factors in nearshore waters, such as tides and river runoff (Cloern,
711 1996). The presence of Delta N15 in the selected environmental variables (Fig. 8B), suggests
712 that agriculture, intensively practiced in our region of interest, could also influence the
713 community structure that we observe at different time of the year.

714 The large contribution of autocorrelation to the variance of the community (Fig. 8C)
715 suggests that intrinsic biological factors (i.e., species interactions, reproductive dynamics,
716 and/or self-regulation of species development; in other words, self-organization properties of
717 the whole biological community; Odum, 1988; Picoche and Barraquand, 2019) are also
718 critical, and significantly contribute to pacing the plankton community. Biotic factors, such as
719 species interactions, partly explain the striking resilience in species turnover also observed
720 for bacterioplankton along a decade (Fuhrman et al., 2015). Microscopic organisms are
721 indeed known to be involved in complex and dynamical networks of interactions (i.e.,
722 grazing, parasitism, mutualism, quorum sensing, etc; Kivi et al., 1993; Dakos et al., 2009;
723 Platt et al., 2009; Bjorbækmo et al., 2020) that are tightly regulating the dynamics of
724 individual species within the whole community structure. Recently, in the WEC at L4 station
725 predator-prey interactions were investigated supporting our hypothesis that they play a role in
726 influencing temporal changes in plankton populations (Barton et al., 2020).

727 Bi-annual variations in the protist community dynamics were also identified from
728 analyses of both dataset (Fig. S4 and Fig. 6). In some ecosystems, rhythmic depletions of
729 resources appear to be at the origin of bimodality (and multimodality) in phytoplankton
730 dynamics (Mellard et al., 2019), however, in our tidally-mixed coastal station, nutrients are
731 never completely depleted (Fig. 2). The bi-annual rhythm could be triggered by the yearly

732 variations of the tidal cycles that are probably at the origin of cycles of enhanced benthic-
733 pelagic coupling; and recently, a reorganization of marine food webs due to strong pelagic-
734 benthic coupling in coastal areas has been reported (Kopp et al., 2015). The number of
735 benthic species detected as prominent in surface waters suggests a tight coupling between
736 benthic and pelagic compartments in the English Channel, which is strengthened in winter,
737 when tidal mixing or winds provoke the resuspension of sediments in the water column.
738 However, in our dbMEM analysis, neither tidal amplitude nor wind appear as a major
739 influential parameter. This yearly bimodality could then be caused by intrinsic plankton
740 biological factors such as endogenous rhythmicity or interactions between species. To better
741 decipher how intrinsic biotic interactions could drive the dynamics of these communities,
742 modelling approaches that take into account biotic interactions (e.g., Picoche and
743 Barraquand, 2019) should be explored, integrating the whole taxonomic and functional
744 spectrum that coexist in space and time, including viruses, prokaryotes, and metazoans.

745

746 **5. Conclusions and perspectives**

747 This study describes the seasonal dynamics of protist communities in a temperate coastal site,
748 complementing early studies (Cushing, 1959; Margalef, 1963; Sommer et al., 1986;
749 Widdicombe et al., 2010) from the same site which considered only diatoms and
750 dinoflagellates. It appears that seasonal successions of protists are primarily paced by
751 astronomical rhythms and may be directly influenced by the resulting temporal variations of
752 the physical and biogeochemical parameters (i.e., PAR, temperature, nutrients, salinity).
753 Intrinsic, plankton self-organization processes are also involved in these annual oscillations.

754 In environments such as the coastal waters of the EC that support one of the busiest shipping
755 lanes in the world, important fishing ports, and an increasing demographic pressure, these
756 seasonal cycles may actually be particularly vulnerable to the combined effects of natural
757 climate variability and local anthropogenic forcing (Dauvin et al. 2008, Tréguer et al. 2014,
758 Gac et al. 2019, Siano 2021). In this context, monitoring activities involving both classical
759 microscopy and metagenomics approaches, such as those conducted along the EC coasts
760 (Breton et al., 2000; Widdicombe et al. 2010; Hernandez-Farinas et al., 2017; Kenitz et al.
761 2017; Käse et al., 2020) should be maintained and developed on the long term. These
762 longitudinal surveys are critical to track and predict future changes that may disrupt the
763 overall resilience of the system, in order to ultimately identify and deploy protective
764 measures to guarantee all the services that these systems provide to the society (Cardinale et
765 al., 2012).

766

767 **Acknowledgements**

768 The authors would like to thank the captains and crew of the Neomysis research ship for their
769 help during sampling at the SOMLIT-Astan station. We are also grateful to the RCC for the
770 maintenance of phytoplankton strains isolated from this station that served for the assignation
771 of some of the genetic sequences. We also thank Cédric Berney and Benjamin Alric for
772 stimulating discussions, and for suggestions to improve the manuscript. Daniel Vaultot is
773 acknowledged for his work on the phytoplankton counts databases. This study was supported
774 by a PhD fellowship from Sorbonne University to MC, the French government research
775 agency programs CALYPSO (ANR-15-CE01-0009), BIOMARKS (“Investissement
776 d’avenir”, ANR-08-BDVA-0003) and OCEANOMICS (ANR-11-BTBR- 0008), the CNRS-

777 INSU EC2CO CYCLOBS research project grant and the Gordon and Betty Moore
778 Foundation through the UniEuk grant GBMF5275.

779 **Authors contributions**

780 NS, FN, NH and MC designed the study. FRJ, TC and the crew of the Neomysis sampled
781 onboard. FRJ and LG produced the taxa counts. MH helped with the construction and
782 maintenance of the phytoplankton counts databases. FRJ, SF and NS contributed to the
783 corrections and validation of the taxonomic counts dataset. FRJ and SR produced the genetic
784 data. TC produced the hydrological data and TC and YB contributed to the validation of the
785 hydrological data validation. JPG produced the final estimations of pH and FCO₂. EG
786 provided the map. SC helped with the calculations of the PAR data. MC and NH analysed the
787 data and produced the scripts and final graphs. MC, NH, ET, FRJ, SR and NS wrote the
788 manuscript. All authors contributed to the discussions that led to the final manuscript, revised
789 it and approved the final version.

790

791 **Data accessibility**

- 792 – Raw environmental data: <https://meteofrance.com/>, <https://www.somlit.fr/en/>,
793 <https://www.somlit.fr/en/>, <https://data.shom.fr/>,
794 <https://modis.gsfc.nasa.gov/data/dataproduct/>, and <https://coastwatch.pfeg.noaa.gov/>
795 – Taxonomic counts input file : <https://doi.org/10.5281/zenodo.5033180>
796 – Metabarcoding raw data: It will be made available after acceptance of the manuscript.
797 – Metabarcoding input file: <https://doi.org/10.5281/zenodo.5032451>

798

799 **References**

- 800 Altenburger, A., Blossom, H. E., Garcia-Cuetos, L., Jakobsen, H. H., Carstensen, J.,
801 Lundholm, N., ... Haraguchi, L. (2020). Dimorphism in cryptophytes—The case of
802 *Teleaulax amphioxeia*/*Plagioselmis prolunga* and its ecological implications. *Science*
803 *Advances*, 6(37), 1–9. <https://doi.org/10.1126/sciadv.abb1611>
- 804 Aminot, A., K erouel R. (2007). Dosage automatique des nutriments dans les eaux marines.
805 M ethodes en flux continu. Ed Ifremer-Quae, 188 p., ISBN-13 978-2-7592-0023-8
- 806 Arsenieff, L., Le Gall, F., Rigaut-Jalabert, F., Mah e, F., Sarno, D., Gouhier, L., ... Simon, N.
807 (2020). Diversity and dynamics of relevant nanoplanktonic diatoms in the Western
808 English Channel. *ISME Journal*, 14(8), 1966–1981. [https://doi.org/10.1038/s41396-020-](https://doi.org/10.1038/s41396-020-0659-6)
809 [0659-6](https://doi.org/10.1038/s41396-020-0659-6)
- 810 Arsenieff, L., Simon, N., Rigaut-Jalabert, F., Le Gall, F., Chaffron, S., Corre, E., ...
811 Baudoux, A. C. (2019). First viruses infecting the marine diatom *Guinardia delicatula*.
812 *Frontiers in Microbiology*, 10(JAN). <https://doi.org/10.3389/fmicb.2018.03235>
- 813 Bar-On, Y. M., & Milo, R. (2019). The Biomass Composition of the Oceans: A Blueprint of
814 Our Blue Planet. *Cell*, 179(7), 1451–1454. <https://doi.org/10.1016/j.cell.2019.11.018>
- 815 Barton, A. D., Lozier, M. S., & Williams, R. G. (2014). Physical controls of variability in
816 North Atlantic phytoplankton communities, 181–197. <https://doi.org/10.1002/lno.10011>
- 817 Barton, A. D., Taboada, F. G., Atkinson, A., Widdicombe, C. E., & Stock, C. A. (2020).
818 Integration of temporal environmental variation by the marine plankton community.
819 *Marine Ecology Progress Series*, 647(Lampert 1989), 1–16.
820 <https://doi.org/10.3354/meps13432>
- 821 Berney, C., Ciuprina, A., Bender, S., Brodie, J., Edgcomb, V., Kim, E., ... de Vargas, C.
822 (2017). UniEuk: Time to Speak a Common Language in Protistology! *Journal of*
823 *Eukaryotic Microbiology*, 64(3), 407–411. <https://doi.org/10.1111/jeu.12414>
- 824 Bivand, R., Wong DWS (2018). “Comparing implementations of global and local indicators
825 of spatial association.” *TEST*, 27(3), 716–748. <https://doi.org/10.1007/s11749-018-0599-x>.
- 826 Bjorb ekmo, M. F. M., Evenstad, A., R os eg, L. L., Krabber od, A. K., & Logares, R. (2020).
827 The planktonic protist interactome: where do we stand after a century of research? *ISME*
828 *Journal*, 14(2), 544–559. <https://doi.org/10.1038/s41396-019-0542-5>
- 829 Boalch, G. T. (1987). Changes in the phytoplankton of the western english channel in recent
830 years. *British Phycological Journal*, 22(3), 225–235.
831 <https://doi.org/10.1080/00071618700650291>
- 832 Bunse, C., & Pinhassi, J. (2017). Marine Bacterioplankton Seasonal Succession Dynamics.
833 *Trends in Microbiology*, 25(6), 494–505. <https://doi.org/10.1016/j.tim.2016.12.013>

- 834 Caracciolo, M., Beaugrand, G., Hélaouët, P., Gevaert, F., Edwards, M., Lizon, F., ...
835 Goberville, E. (2021). Annual phytoplankton succession results from niche-environment
836 interaction. *Journal of Plankton Research*, 43(1), 85–102.
837 <https://doi.org/10.1093/plankt/fbaa060>
- 838 Cardinale, B. J., Duffy, J. E., Gonzalez, A., Hooper, D. U., Perrings, C., Venail, P., ...
839 Naeem, S. (2012). Biodiversity loss and its impact on humanity. *Nature*, 486(7401), 59–
840 67. <https://doi.org/10.1038/nature11148>
- 841 Chambouvet, A., Morin, P., Marie, D., & Guillou, L. (2008). Control of toxic marine
842 dinoflagellate blooms by serial parasitic killers. *Science*, 322(5905), 1254–1257.
843 <https://doi.org/10.1126/science.1164387>
- 844 Cloern, J. E. (1996). Phytoplankton bloom dynamics in coastal ecosystems: A review with
845 some general lessons from sustained investigation of San Francisco Bay, California.
846 *Reviews of Geophysics*, 34(2), 127–168. <https://doi.org/10.1029/96RG00986>
- 847 Cottingham, K. L., Brown, B. L., & Lennon, J. T. (2001). Biodiversity may regulate the
848 temporal variability of ecological systems. *Ecology Letters*, 4(1), 72–85.
849 <https://doi.org/10.1046/j.1461-0248.2001.00189.x>
- 850 Craine, J. M., Wolkovich, E. M., & Towne, E. G. (2012). The roles of shifting and filtering in
851 generating community-level flowering phenology. *Ecography*, 35(11), 1033–1038.
852 <https://doi.org/10.1111/j.1600-0587.2012.07625.x>
- 853 Crawford, D., & Purdie, D. (1991). Evidence for avoidance of flushing from an estuary by a
854 planktonic, phototrophic ciliate. *Marine Ecology Progress Series*, 79(January), 259–265.
855 <https://doi.org/10.3354/meps079259>
- 856 Cushing, D. H. (1959). The seasonal variation in oceanic production as a problem in
857 population dynamics. *ICES Journal of Marine Science*, 24(3), 455–464.
858 <https://doi.org/10.1093/icesjms/24.3.455>
- 859 Cushing, D. H. (1990). Plankton production and year-class strength in fish populations: An
860 update of the match/mismatch hypothesis. *Advances in Marine Biology* (Vol. 26).
861 [https://doi.org/10.1016/S0065-2881\(08\)60202-3](https://doi.org/10.1016/S0065-2881(08)60202-3)
- 862 Dakos, V., Benincà, E., van Nes, E. H., Philippart, C. J. M., Scheffer, M., & Huisman, J.
863 (2009). Interannual variability in species composition explained as seasonally entrained
864 chaos. *Proceedings. Biological Sciences / The Royal Society*, 276(1669), 2871–2880.
865 <https://doi.org/10.1098/rspb.2009.0584>
- 866 Dauvin, J. C. (2008). The main characteristics, problems, and prospects for Western
867 European coastal seas. *Marine Pollution Bulletin*, 57(1–5), 22–40.
868 <https://doi.org/10.1016/j.marpolbul.2007.10.016>

- 869 Delavenne, J., Marchal, P., & Vaz, S. (2013). Defining a pelagic typology of the eastern
870 English Channel. *Continental Shelf Research*, 52(January), 87–96.
871 <https://doi.org/10.1016/j.csr.2012.10.016>
- 872 Dickie, P. M. (2001). *Flow Cytometry*, 246, 236–246.
- 873 Drake, J. A. (1990). The mechanics of community assembly and succession. *Journal of*
874 *Theoretical Biology*, 147(2), 213–233. [https://doi.org/10.1016/S0022-5193\(05\)80053-0](https://doi.org/10.1016/S0022-5193(05)80053-0)
- 875 Dray, S., & Dufour, A. B. (2007). The ade4 package: Implementing the duality diagram for
876 ecologists. *Journal of Statistical Software*, 22(4), 1–20.
877 <https://doi.org/10.18637/jss.v022.i04>
- 878 Dray, S., Blanchet, G., Borcard, D., Guenard, G., Jombart, T., Larocque, G., ... Dray, M.
879 (2018). Package “adespatial.” *R Package Version*, 3–8. [https://doi.org/10.1890/11-](https://doi.org/10.1890/11-1183.1)
880 [1183.1](https://doi.org/10.1890/11-1183.1).Maintainer
- 881 Drebes, G., Kühn, S. F., Gmelch, A., & Schnepf, E. (1996). *Cryothecomonas aestivalis* sp.
882 nov., a colourless nanoflagellate feeding on the marine centric diatom *Guinardia*
883 *delicatula* (Cleve) Hasle. *Helgolander Meeresuntersuchungen*, 50(4), 497–515.
884 <https://doi.org/10.1007/bf02367163>
- 885 Edwards, K. F., Litchman, E., & Klausmeier, C. A. (2013). Functional traits explain
886 phytoplankton community structure and seasonal dynamics in a marine ecosystem.
887 *Ecology Letters*, 16(1), 56–63. <https://doi.org/10.1111/ele.12012>
- 888 Edwards, M., & Richardson, A. J. (2003). Impact of climate change on marine pelagic
889 phenology and. *Nature*, 4030(7002), 881.
- 890 Egge, E. S., Johannessen, T. V., Andersen, T., Eikrem, W., Bittner, L., Larsen, A., ...
891 Edvardsen, B. (2015). Seasonal diversity and dynamics of haptophytes in the Skagerrak,
892 Norway, explored by high-throughput sequencing. *Molecular Ecology*, 24(12), 3026–
893 3042. <https://doi.org/10.1111/mec.13160>
- 894 Forster, D., Dunthorn, M., Mahé, F., Dolan, J. R., Audic, S., Bass, D., ... Stoeck, T. (2016).
895 Benthic protists: The under-charted majority. *FEMS Microbiology Ecology*, 92(8), 2–33.
896 <https://doi.org/10.1093/femsec/fiw120>
- 897 Foulon, E., Not, F., Jalabert, F., Cariou, T., Massana, R., & Simon, N. (2008). Ecological
898 niche partitioning in the picoplanktonic green alga *Micromonas pusilla*: Evidence from
899 environmental surveys using phylogenetic probes. *Environmental Microbiology*, 10(9),
900 2433–2443. <https://doi.org/10.1111/j.1462-2920.2008.01673.x>
- 901 Fuhrman, J. A., Hewson, I., Schwalbach, M. S., Steele, J. A., Brown, M. V., & Naeem, S.
902 (2006). Annually reoccurring bacterial communities are predictable from ocean

- 903 conditions. *Proceedings of the National Academy of Sciences*, *103*(35), 13104–13109.
904 <https://doi.org/10.1073/pnas.0602399103>
- 905 Fuhrman, J. A. (2009). Microbial community structure and its functional implications,
906 *459*(May). <https://doi.org/10.1038/nature08058>
- 907 Fuhrman, J. A., Cram, J. A., & Needham, D. M. (2015). Marine microbial community
908 dynamics and their ecological interpretation. *Nature Reviews: Microbiology*, *13*(3), 133–
909 146. <https://doi.org/10.1038/nrmicro3417>
- 910 Gac, J. P., Marrec, P., Cariou, T., Guillerm, C., Macé, É., Vernet, M., & Bozec, Y. (2020).
911 Cardinal Buoys: An Opportunity for the Study of Air-Sea CO₂ Fluxes in Coastal
912 Ecosystems. *Frontiers in Marine Science*, *7*(August), 1–21.
913 <https://doi.org/10.3389/fmars.2020.00712>
- 914 Genner, M. J., Sims, D. W., Wearmouth, V. J., Southall, E. J., Southward, A. J., Henderson,
915 P. A., & Hawkins, S. J. (2004). Regional climatic warming drives long-term community
916 changes of British marine fish. *Proceedings of the Royal Society B: Biological Sciences*,
917 *271*(1539), 655–661. <https://doi.org/10.1098/rspb.2003.2651>
- 918 Gilbert, J. A., Steele, J. A., Caporaso, J. G., Steinbrück, L., Reeder, J., Temperton, B., ...
919 Field, D. (2012). Defining seasonal marine microbial community dynamics. *ISME*
920 *Journal*, *6*(2), 298–308. <https://doi.org/10.1038/ismej.2011.107>
- 921 Giner, C. R., Balagué, V., Krabberød, A. K., Ferrera, I., Reñé, A., Garcés, E., ... Massana, R.
922 (2019). Quantifying long-term recurrence in planktonic microbial eukaryotes. *Molecular*
923 *Ecology*, *28*(5), 923–935. <https://doi.org/10.1111/mec.14929>
- 924 Glöckner, F. O., Yilmaz, P., Quast, C., Gerken, J., Beccati, A., Ciuprina, A., ... Ludwig, W.
925 (2017). 25 years of serving the community with ribosomal RNA gene reference
926 databases and tools. *Journal of Biotechnology*, *261*(February), 169–176.
927 <https://doi.org/10.1016/j.jbiotec.2017.06.1198>
- 928 Gómez, F., & Souissi, S. (2007). Unusual diatoms linked to climatic events in the
929 northeastern English Channel. *Journal of Sea Research*, *58*(4), 283–290.
930 <https://doi.org/10.1016/j.seares.2007.08.002>
- 931 Gong, W., & Marchetti, A. (2019). Estimation of 18S gene copy number in marine eukaryotic
932 plankton using a next-generation sequencing approach. *Frontiers in Marine Science*,
933 *6*(APR), 1–5. <https://doi.org/10.3389/fmars.2019.00219>
- 934 Grall, J. R. (1972). Développement “printanier” de la diatomée *Rhizosolenia delicatula* près
935 de Roscoff. *Marine Biology*, *16*(1), 41–48. <https://doi.org/10.1007/BF00347846>

- 936 Griffin, J. N., O’Gorman, E. J., Emmerson, M. C., Jenkins, S. R., Klein, A. M., Loreau, M.,
937 & Symstad, A. (2009). Biodiversity and the stability of ecosystem functioning.
938 *Biodiversity, Ecosystem Functioning, and Human Wellbeing: An Ecological and*
939 *Economic Perspective*. <https://doi.org/10.1093/acprof:oso/9780199547951.003.0006>
- 940 Guilloux, L., Rigaut-Jalabert, F., Jouenne, F., Ristori, S., Viprey, M., Not, F., ... Simon, N.
941 (2013). An annotated checklist of Marine Phytoplankton taxa at the SOMLIT-Astan
942 time series off Roscoff (Western English Channel, France): Data collected from 2000 to
943 2010. *Cahiers de Biologie Marine*, 54(2), 247–256.
944 <https://doi.org/10.21411/cbm.a.a7f4d2e6>
- 945 Hartley, B., Barber H. & Carter J. 1996. An atlas of british diatoms. Biopress Ltd. England &
946 Natural History Museum: 601 pp.
- 947 Henry N., Caracciolo M., Mahé F., Romac S., Rigaut-Jalabert F., & Simon N. (2021). V4
948 rDNA sequences organized at the OTU level for the SOMLIT-Astan time-series (2009-2016)
949 (Version First version) [Data set]. Zenodo. <http://doi.org/10.5281/zenodo.5032451>
- 950 Hernández-Fariñas, T., Soudant, D., Barille´, L., Belin, C., Lefebvre, A., and Bacher, C.
951 (2014). Temporal changes in the phytoplankton community along the French coast of
952 the eastern English Channel and the southern Bight of the North Sea.–*ICES Journal of*
953 *Marine Science*, 71: 821–833.
- 954 Hernández Fariñas, T., Ribeiro, L., Soudant, D., Belin, C., Bacher, C., Lampert, L., & Barillé,
955 L. (2017). Contribution of benthic microalgae to the temporal variation in phytoplankton
956 assemblages in a macrotidal system. *Journal of Phycology*, 53(5), 1020–1034.
957 <https://doi.org/10.1111/jpy.12564>
- 958 Hoppenrath M., Elbrächter M. & Drebes G. (2009). Marine phytoplankton: Selected
959 microphytoplankton species from the North Sea around Helgoland and Sylt. *Kleine*
960 *SenckenbergReihe*, 49: Stuttgart. 264 pp.
- 961 Horner, R. (2002). Taxonomic guide to some common marine phytoplankton. Biopress:
962 Dorchester. 195 pp.
- 963 Hiscock, K., Southward, A., Tittley, I., & Hawkins, S. (2004). Effects of changing
964 temperature on benthic marine life in Britain and Ireland. *Aquatic Conservation: Marine*
965 *and Freshwater Ecosystems*, 14(4), 333–362. <https://doi.org/10.1002/aqc.628>
- 966 Hurrell, J. W. (1995). Decadal trends in the North Atlantic oscillation: Regional temperatures
967 and precipitation. *Science*, 269(5224), 676–679.
968 <https://doi.org/10.1126/science.269.5224.676>
- 969 Käse, L., Kraberg, A. C., Metfies, K., Neuhaus, S., Sprong, P. A. A., Fuchs, B. M., ...
970 Wiltshire, K. H. (2020). Rapid succession drives spring community dynamics of small

- 971 protists at Helgoland Roads, North Sea. *Journal of Plankton Research*, 42(3), 305–319.
972 <https://doi.org/10.1093/plankt/fbaa017>
- 973 Kivi, K., Kaitala, S., Kuosa, H., Kuparinen, J., Leskinen, E., Lignell, R., ... Tamminen, T.
974 (1993). Nutrient limitation and grazing control of the Baltic plankton community during
975 annual succession. *Limnology and Oceanography*, 38(5), 893–905.
976 <https://doi.org/10.4319/lo.1993.38.5.0893>
- 977 Kopp, D., Lefebvre, S., Cachera, M., Villanueva, M. C., & Ernande, B. (2015).
978 Reorganization of a marine trophic network along an inshore-offshore gradient due to
979 stronger pelagic-benthic coupling in coastal areas. *Progress in Oceanography*,
980 130(January), 157–171. <https://doi.org/10.1016/j.pocean.2014.11.001>
- 981 Kraberg, A., Baumann M. & Dürselen C.-D. 2010. Coastal phytoplankton: photo guide for
982 Northern European Seas. Verlag Dr. Friedrich Pfeil: München. 204 p.
- 983 Lambert, S., Tragin, M., Lozano, J. C., Ghiglione, J. F., Vaultot, D., Bouget, F. Y., & Galand,
984 P. E. (2019). Rhythmicity of coastal marine picoeukaryotes, bacteria and archaea despite
985 irregular environmental perturbations. *ISME Journal*, 13(2), 388–401.
986 <https://doi.org/10.1038/s41396-018-0281-z>
- 987 Leblanc, K., Quéguiner, B., Diaz, F., Cornet, V., Michel-rodriguez, M., Madron, X. D. De,
988 ... Conan, P. (2018). but play a role in spring blooms and carbon export. *Nature*
989 *Communications*, 1–12. <https://doi.org/10.1038/s41467-018-03376-9>
- 990 Legendre, P. and Legendre, L. (1998) *Numerical Ecology*, 2nd English edn,
991 Elsevier Amsterdam.
- 992 Legendre, P., & Gallagher, E. D. (2001). Ecologically meaningful transformations for
993 ordination of species data. *Oecologia*, 129(2), 271–280.
994 <https://doi.org/10.1007/s004420100716>
- 995 Legendre, P., & Gauthier, O. (2014). Statistical methods for temporal and space-time analysis
996 of community composition data. *Proceedings of the Royal Society B: Biological*
997 *Sciences*, 281(1778). <https://doi.org/10.1098/rspb.2013.2728>
- 998 Legendre, P., Oksanen, J., & ter Braak, C. J. F. (2011). Testing the significance of canonical
999 axes in redundancy analysis. *Methods in Ecology and Evolution*, 2(3), 269–277.
1000 <https://doi.org/10.1111/j.2041-210X.2010.00078.x>
- 1001 Leterme, S. C., Edwards, M., Seuront, L., Attrill, M. J., Reid, P. C., & John, A. W. G. (2005).
1002 Decadal basin-scale changes in diatoms, dinoflagellates, and phytoplankton color across
1003 the North Atlantic. *Limnology and Oceanography*, 50(4), 1244–1253.
1004 <https://doi.org/10.4319/lo.2005.50.4.1244>

- 1005 L'Helguen, S., Madec, C., & Corre, P. Le. (1996). Nitrogen uptake in permanently well-
1006 mixed temperate coastal waters. *Estuarine, Coastal and Shelf Science*, 42(6), 803–818.
1007 <https://doi.org/10.1006/ecss.1996.0051>
- 1008 Logares, R., Tesson, S. V. M., Canbäck, B., Pontarp, M., Hedlund, K., & Rengefors, K.
1009 (2018). Contrasting prevalence of selection and drift in the community structuring of
1010 bacteria and microbial eukaryotes. *Environmental Microbiology*, 20(6), 2231–2240.
1011 <https://doi.org/10.1111/1462-2920.14265>
- 1012 Longhurst, A. 1998. *Ecological Geography of the Sea*. San Diego, Academic Press.
- 1013 Loreau, M., Naeem, S., Inchausti, P., Bengtsson, J., Grime, J. P., Hector, A., ... Wardle, D.
1014 A. (2001). Ecology: Biodiversity and ecosystem functioning: Current knowledge and
1015 future challenges. *Science*, 294(5543), 804–808.
1016 <https://doi.org/10.1126/science.1064088>
- 1017 Loreau, M., & de Mazancourt, C. (2013). Biodiversity and ecosystem stability: A synthesis of
1018 underlying mechanisms. *Ecology Letters*, 16(SUPPL.1), 106–115.
1019 <https://doi.org/10.1111/ele.12073>
- 1020 Mahé, F., Rognes, T., Quince, C., de Vargas, C., & Dunthorn, M. (2014). Swarm: robust and
1021 fast clustering method for amplicon-based studies. *PeerJ*, 2, e593.
1022 <https://doi.org/10.7717/peerj.593>
- 1023 Mahé, F., Rognes, T., Quince, C., de Vargas, C., & Dunthorn, M. (2015). Swarm v2: highly-
1024 scalable and high-resolution amplicon clustering. *PeerJ*, 3, e1420.
1025 <https://doi.org/10.7717/peerj.1420>
- 1026 Mann, K. and Lazier, J. (1991) Dynamics of Marine Ecosystems
- 1027 Margalef, R. (1963). On Certain Unifying Principles in Ecology. *The American Naturalist*,
1028 97(897), 357–374. <https://doi.org/10.1086/282286>
- 1029 Margalef, R. (1958). „Trophic” typology versus biotic typology, as exemplified in the
1030 regional limnology of Northern Spain. *SIL Proceedings, 1922-2010*, 13(1), 339–349.
1031 <https://doi.org/10.1080/03680770.1956.11895414>
- 1032 Marquardt, M., Vader, A., Stübner, E. I., Reigstad, M., & Gabrielsen, T. M. (2016). Strong
1033 seasonality of marine microbial eukaryotes in a high-Arctic fjord (Isfjorden, in West
1034 Spitsbergen, Norway). *Applied and Environmental Microbiology*, 82(6), 1868–1880.
1035 <https://doi.org/10.1128/AEM.03208-15>
- 1036 Martin-Jezequel, V. (1983). Facteurs hydrologiques et phytoplancton en Baie de Morlaix
1037 (Manche Occidentale). *Hydrobiologia*, 102(2), 131–143.
1038 <https://doi.org/10.1007/bf00006076>

- 1039 Martin-jézéquel, V., Sournia, A., & Birrien, J. L. (1992). A daily study of the diatom spring
1040 bloom at Roscoff (France) in 1985. III. Free amino acids composition studied by HPLC
1041 analysis. *Journal of Plankton Research*, *14*(3), 409–421.
1042 <https://doi.org/10.1093/plankt/14.3.409>
- 1043 McCook, L. J. (1994). Understanding ecological community succession: Causal models and
1044 theories, a review. *Vegetatio*, *110*(2), 115–147. <https://doi.org/10.1007/BF00033394>
- 1045 Mellard, J. P., Audoye, P., & Loreau, M. (2019). Seasonal patterns in species diversity across
1046 biomes. *Ecology*, *100*(4), e02627. <https://doi.org/10.1002/ecy.2627>
- 1047 Mieszkowska, N., Burrows, M. T., Pannacciulli, F. G., & Hawkins, S. J. (2014). Multidecadal
1048 signals within co-occurring intertidal barnacles *Semibalanus balanoides* and *Chthamalus*
1049 spp. linked to the Atlantic Multidecadal Oscillation. *Journal of Marine Systems*, *133*,
1050 70–76. <https://doi.org/10.1016/j.jmarsys.2012.11.008>
- 1051 Millette, N. C., Pierson, J. J., Aceves, A., & Stoecker, D. K. (2017). Mixotrophy in
1052 *Heterocapsa rotundata*: A mechanism for dominating the winter phytoplankton.
1053 *Limnology and Oceanography*, *62*(2), 836–845. <https://doi.org/10.1002/lno.10470>
- 1054 Modigh, M. (2001). Seasonal variations of photosynthetic ciliates at a Mediterranean coastal
1055 site. *Aquatic Microbial Ecology*, *23*(2), 163–175. <https://doi.org/10.3354/ame023163>
- 1056 Molinero, J. C., Reygondeau, G., & Bonnet, D. (2013). Climate variance influence on the
1057 non-stationary plankton dynamics. *Marine Environmental Research*, *89*, 91–96.
1058 <https://doi.org/10.1016/j.marenvres.2013.04.006>
- 1059 Moran, M. A. (2015). The global ocean microbiome. *Science*, *350*(6266).
1060 <https://doi.org/10.1126/science.aac8455>
- 1061 Not, F., Latasa, M., Marie, D., Cariou, T., Vaultot, D., & Simon, N. (2004). A single species,
1062 *Micromonas pusilla* (Prasinophyceae), dominates the eukaryotic picoplankton in the
1063 Western English Channel. *Applied and Environmental Microbiology*, *70*(7), 4064–4072.
1064 <https://doi.org/10.1128/AEM.70.7.4064-4072.2004>
- 1065 Oksanen, A. J., Blanchet, F. G., Friendly, M., Kindt, R., Legendre, P., Mcglinn, D., ...
1066 Szocs, E. (2013). Package ‘vegan’, (December 2016), 0–291.
- 1067 Falkowski, P. G., Fenchel, T. & Delong, E. F. (2008). The Microbial Engines That Drive
1068 Earth’s Biogeochemical Cycles. *Science*, *320*(5879), 1034–1039.
1069 <https://doi.org/10.1126/science.1153213>
- 1070 Paradis, E., & Schliep, K. (2019). Ape 5.0: An environment for modern phylogenetics and
1071 evolutionary analyses in R. *Bioinformatics*, *35*(3), 526–528.
1072 <https://doi.org/10.1093/bioinformatics/bty633>

- 1073 Patterson, D.J., Larsen, J., Corliss, J.O. (1989) The ecology of heterotrophic flagellates and
1074 ciliates living in marine sediments. *Prog Protistol* 1989;3:185–277.
- 1075 Peacock, E. E., Olson, R. J., & Sosik, H. M. (2014). Parasitic infection of the diatom
1076 *Guinardia delicatula*, a recurrent and ecologically important phenomenon on the New
1077 England Shelf. *Marine Ecology Progress Series*, 503, 1–10.
1078 <https://doi.org/10.3354/meps10784>
- 1079 Percopo, I., Siano, R., Cerino, F., Sarno, D., & Zingone, A. (2011). Phytoplankton diversity
1080 during the spring bloom in the northwestern Mediterranean Sea. *Botanica Marina*,
1081 54(3), 243–267. <https://doi.org/10.1515/BOT.2011.033>
- 1082 Picoche, C., & Barraquand, F. (2019). How self-regulation, the storage effect, and their
1083 interaction contribute to coexistence in stochastic and seasonal environments.
1084 *Theoretical Ecology*, 12(4), 489–500. <https://doi.org/10.1007/s12080-019-0420-9>
- 1085 Pingree, R. D., & Griffiths, D. K. (1978). Tidal fronts on the shelf seas around the British
1086 Isles. *Journal of Geophysical Research*, 83(C9), 4615.
1087 <https://doi.org/10.1029/jc083ic09p04615>
- 1088 Pingree, R. D., & Griffiths, D. K. (1980). Currents driven by a steady uniform wind stress on
1089 the shelf seas around the British Isles. *Oceanologica Acta*, 3(2), 227–236.
- 1090 Piredda, R., Tomasino, M. P., D’Erchia, A. M., Manzari, C., Pesole, G., Montresor, M., ...
1091 Zingone, A. (2017). Diversity and temporal patterns of planktonic protist assemblages at
1092 a Mediterranean Long Term Ecological Research site. *FEMS Microbiology Ecology*,
1093 93(1), 1–14. <https://doi.org/10.1093/femsec/fiw200>
- 1094 Platt, T., Sathyendranath, S., White, G. N., Fuentes-Yaco, C., Zhai, L., Devred, E., & Tang,
1095 C. (2010). Diagnostic properties of phytoplankton time series from remote sensing.
1096 *Estuaries and Coasts*, 33(2), 428–439. <https://doi.org/10.1007/s12237-009-9161-0>
- 1097 Qiu, D., Huang, L., & Lin, S. (2016). Cryptophyte farming by symbiotic ciliate host detected
1098 in situ. *Proceedings of the National Academy of Sciences of the United States of*
1099 *America*, 113(43), 12208–12213. <https://doi.org/10.1073/pnas.1612483113>
- 1100 Reygondeau, G., Molinero, J. C., Coombs, S., MacKenzie, B. R., & Bonnet, D. (2015).
1101 Progressive changes in the Western English Channel foster a reorganization in the
1102 plankton food web. *Progress in Oceanography*, 137, 524–532.
1103 <https://doi.org/10.1016/j.pocean.2015.04.025>
- 1104 Reynolds, C.S. (1984). Phytoplankton periodicity: the interactions of form , function and
1105 environmental variability. *Freshwater Biology*, 14, 111–142.

- 1106 Ribera d'Alcalà, M., Conversano, F., Corato, F., Licandro, P., Mangoni, O., Marino, D., ...
1107 Zingone, A. (2004). Seasonal patterns in plankton communities in pluriannual time
1108 series at a coastal Mediterranean site (Gulf of Naples): An attempt to discern recurrences
1109 and trends. *Scientia Marina*, 68(SUPPL 1), 65–83.
1110 <https://doi.org/10.3989/scimar.2004.68s165>
- 1111 Richardson, A. D., Black, T. A., Ciais, P., Delbart, N., Friedl, M. A., Gobron, N., ...
1112 Varlagin, A. (2010). Influence of spring and autumn phenological transitions on forest
1113 ecosystem productivity. *Philosophical Transactions of the Royal Society B: Biological*
1114 *Sciences*, 365(1555), 3227–3246. <https://doi.org/10.1098/rstb.2010.0102>
- 1115 Rigaut-Jalabert F., Guilloux L, Hoebeke M., Forsans S., Caracciolo M., & Simon N. (2021).
1116 Morphological phytoplankton counts for the SOMLIT-Astan time-series (2007-2017)
1117 (Version Version 1) [Data set]. Zenodo. <http://doi.org/10.5281/zenodo.5033180>
- 1118 Robbins, P. (2014). Marine Science. *Encyclopedia of Environment and Society*, 71, 821–833.
1119 <https://doi.org/10.4135/9781412953924.n678>
- 1120 Rognes, T., Flouri, T., Nichols, B., Quince, C., & Mahé, F. (2016). VSEARCH: A versatile
1121 open source tool for metagenomics. *PeerJ*, 2016(10), 1–22.
1122 <https://doi.org/10.7717/peerj.2584>
- 1123 Sambrook, J., E. F. Fritsch, and T. Maniatis. (1989). *Molecular cloning: a laboratory Manual*,
1124 2nd ed., Cold Spring Harbor Laboratory Press, Cold Spring Harbor, N.Y.
- 1125 Santi, I., Kasapidis, P., Karakassis, I., & Pitta, P. (2021). A comparison of DNA
1126 metabarcoding and microscopy methodologies for the study of aquatic microbial
1127 eukaryotes. *Diversity*, 13(5), 1–12. <https://doi.org/10.3390/d13050180>
- 1128 Schlüter, U., Mascher, M., Colmsee, C., Scholz, U., Bräutigam, A., Fahnenstich, H., &
1129 Sonnewald, U. (2012). Maize source leaf adaptation to nitrogen deficiency affects not
1130 only nitrogen and carbon metabolism but also control of phosphate homeostasis. *Plant*
1131 *Physiology*, 160(3), 1384–1406. <https://doi.org/10.1104/pp.112.204420>
- 1132 Siano, R., Lassudrie, M., Cuzin, P., Briant, N., Loizeau, V., Schmidt, S., ... Penaud, A.
1133 (2021). Sediment archives reveal irreversible shifts in plankton communities after World
1134 War II and agricultural pollution. *Current Biology*, 1–8.
1135 <https://doi.org/10.1016/j.cub.2021.03.079>
- 1136 Smetacek, V. S. (1985). Role of sinking in diatom life-history cycles: ecological,
1137 evolutionary and geological significance. *Marine Biology*, 84(3), 239–251.
1138 <https://doi.org/10.1007/BF00392493>
- 1139 Sommer, U., Gliwicz, Z., Lampert, W. and Duncan, A. (1986) The PEG model
1140 of seasonal succession of planktonic events in fresh waters. *Arch. Hydrobiol.*, **106**, 433–471.

- 1141 Sommer, U., Adrian, R., De Senerpont Domis, L., Elser, J. J., Gaedke, U., Ibelings, B., ...
1142 Winder, M. (2012). Beyond the plankton ecology group (PEG) model: Mechanisms
1143 driving plankton succession. *Annual Review of Ecology, Evolution, and Systematics*, *43*,
1144 429–448. <https://doi.org/10.1146/annurev-ecolsys-110411-160251>
- 1145 Southward, A. J., Langmead, O., Hardman-Mountford, N. J., Aiken, J., Boalch, G. T., Dando,
1146 P. R., ... Hawkins, S. J. (2004). *Long-term oceanographic and ecological research in*
1147 *the western English Channel. Advances in Marine Biology* (Vol. 47).
1148 [https://doi.org/10.1016/S0065-2881\(04\)47001-1](https://doi.org/10.1016/S0065-2881(04)47001-1)
- 1149 Spongiaires, D. E. S., Roscoff, D. E., & Région, D. E. L. A. (1968). Contribution a la
1150 connaissance Louis Cabioch Roscoff : *Dercitus bucklandi* , *Suberites carnosus* ,
1151 *Axinella dissimilis* , *Ulosa digitata* , *Hymedesmia versicolor* . Le Professeur Claude
1152 Levi s ' est intéressé à mon travail et a vérifié l ' exactitud.
- 1153 Stoeck, T., Bass, D., Nebel, M., Christen, R., & Meredith, D. (2010). Multiple marker
1154 parallel tag environmental DNA sequencing reveals a highly complex eukaryotic
1155 community in marine anoxic water, *19*, 21–31. [https://doi.org/10.1111/j.1365-](https://doi.org/10.1111/j.1365-294X.2009.04480.x)
1156 [294X.2009.04480.x](https://doi.org/10.1111/j.1365-294X.2009.04480.x)
- 1157 Sverdrup, H. U. (1953). On conditions for the vernal blooming of phytoplankton. *ICES*
1158 *Journal of Marine Science*, *18*(3), 287–295. <https://doi.org/10.1093/icesjms/18.3.287>
- 1159 Throndsen, J., Hasle, G. & Tangen, K. (2007). Phytoplankton of Norwegian coastal waters.
1160 Almater forlag AS: Oslo. 343 pp
- 1161 Tilman, D., Reich, P. B., & Knops, J. M. H. (2006). Biodiversity and ecosystem stability in a
1162 decade-long grassland experiment. *Nature*, *441*(7093), 629–632.
1163 <https://doi.org/10.1038/nature04742>
- 1164 Tomas, C. R. (ed.) (1997) *Identifying Marine Phytoplankton*. Academic Press, San Diego,
1165 CA.
- 1166 Townsend, D. W., Keller, M. D., Sieracki, M. E., & Acklesont, S. G. (1992). Column
1167 Stratification, *360*(November), 59–62.
- 1168 Townsend, D. W., Cammen, L. M., Holligan, P. M., Campbell, D. E., & Pettigrew, N. R.
1169 (1994). Causes and consequences of variability in the timing of spring phytoplankton blooms.
1170 *Deep-Sea Research Part I*, *41*(5–6), 747–765. [https://doi.org/10.1016/0967-0637\(94\)90075-2](https://doi.org/10.1016/0967-0637(94)90075-2)
- 1171 Tréguer, P., Goberville, E., Barrier, N., L'Helguen, S., Morin, P., Bozec, Y., ... Quémener, L.
1172 (2014). Large and local-scale influences on physical and chemical characteristics of
1173 coastal waters of Western Europe during winter. *Journal of Marine Systems*,
1174 *139*(November), 79–90. <https://doi.org/10.1016/j.jmarsys.2014.05.019>

- 1175 Trigo, R. M., Osborn, T. J., & Corte-Real, J. M. (2002). The North Atlantic Oscillation
1176 influence on Europe: Climate impacts and associated physical mechanisms. *Climate*
1177 *Research*, 20(1), 9–17. <https://doi.org/10.3354/cr020009>
- 1178 Villarino, E., Watson, J. R., Jönsson, B., Gasol, J. M., Salazar, G., Acinas, S. G., ... Chust, G.
1179 (2018). Large-scale ocean connectivity and planktonic body size. *Nature*
1180 *Communications*, 9(1). <https://doi.org/10.1038/s41467-017-02535-8>
- 1181 Wafar, M. V. M., Le Corre, P., & Birrien, J. L. (1983). Nutrients and primary production in
1182 permanently well-mixed temperate coastal waters. *Estuarine, Coastal and Shelf Science*,
1183 17(4), 431–446. [https://doi.org/10.1016/0272-7714\(83\)90128-2](https://doi.org/10.1016/0272-7714(83)90128-2)
- 1184 Wickham, H. (2016). ggplot2 Elegant Graphics for Data Analysis (Use R!). *Springer*, 213.
1185 Retrieved from <http://had.co.nz/ggplot2/book>
- 1186 Widdicombe, C. E., Eloire, D., & Harbour, D. (2010). Long-term phytoplankton community
1187 dynamics in the Western English Channel, 32. <https://doi.org/10.1093/plankt/fbp127>
- 1188 Wiltshire, K. H., Malzahn, A. M., Wirtz, K., Greve, W., Janisch, S., Mangelsdorf, P., ...
1189 Boersma, M. (2008). Resilience of North Sea phytoplankton spring bloom dynamics: An
1190 analysis of long-term data at Helgoland Roads. *Limnology and Oceanography*, 53(4),
1191 1294–1302. <https://doi.org/10.4319/lo.2008.53.4.1294>
- 1192 Winder, M., & Cloern, J. E. (2010). The annual cycles of phytoplankton biomass.
1193 *Philosophical Transactions of the Royal Society B: Biological Sciences*, 365(1555),
1194 3215–3226. <https://doi.org/10.1098/rstb.2010.0125>
- 1195 Zhai, L., Platt, T., Tang, C., Sathyendranath, S., & Walne, A. (2013). The response of
1196 phytoplankton to climate variability associated with the North Atlantic Oscillation.
1197 *Deep-Sea Research Part II: Topical Studies in Oceanography*, 93, 159–168.
1198 <https://doi.org/10.1016/j.dsr2.2013.04.009>

Figure 1

Location of the study area. The SOMLIT-Astan sampling station (48:46'49" N; 3:58'14" W) is located in the Western English Channel, 3.5 km from the coast. The water column at this site is 60 m deep and is never stratified due to intense tidal mixing. The site is strongly impacted by storms in Winter.

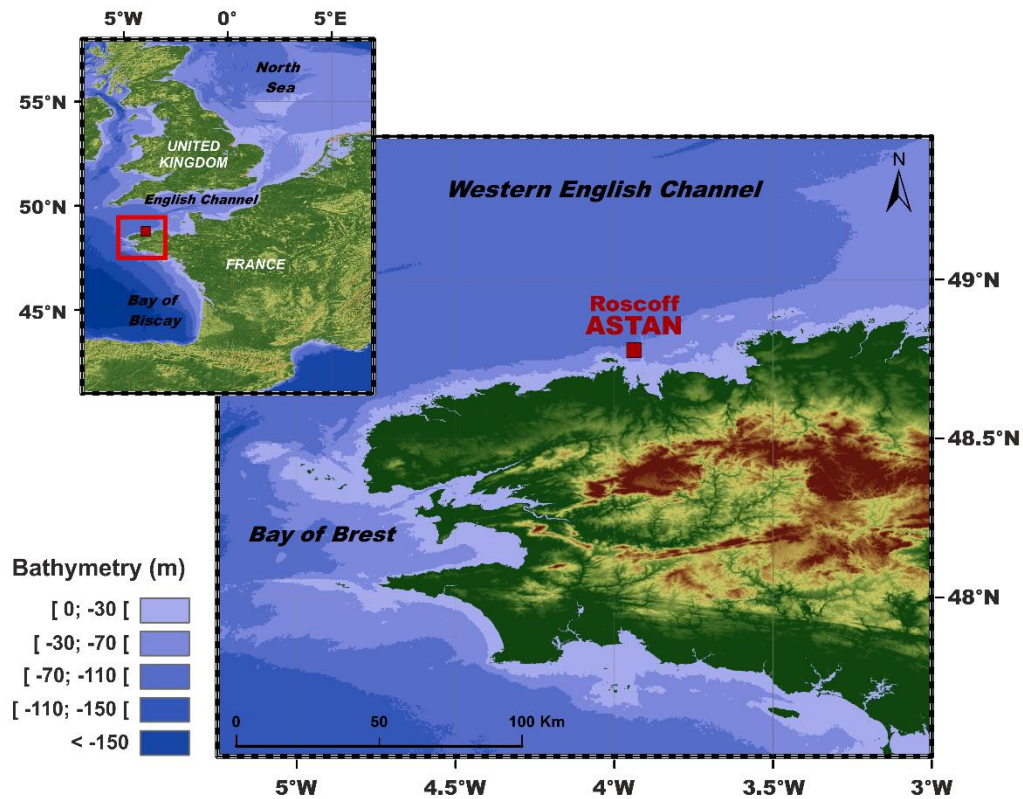


Figure 2

Monthly variations of the hydrological and meteorological parameters at the SOMLIT-Astan time-series station in the period 2009-2016. Sampling was carried out at high neap tides. PAR is the photosynthetically available radiation calculated as the average light received during the 8 days before sampling. Kd490 is intended as the diffuse attenuation coefficient for downwelling irradiance at 490 nm. Interannual variations of all parameters presented in this figure can be found in figure S2.

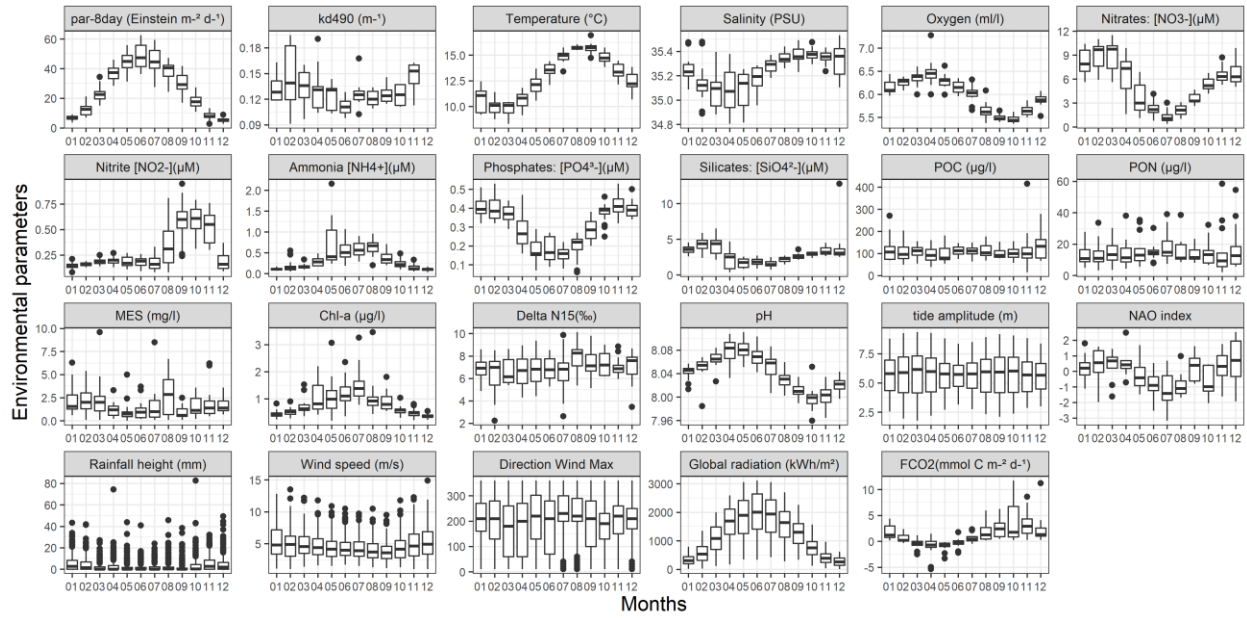


Figure 3

Changes in alpha and beta diversity calculated for the protist assemblages over the period 2009-2016 at the SOMLIT-Astan sampling station. (A, B): Seasonal variations in the Shannon Indexes calculated for the period 2009-2016. **(C, D):** Interannual recurrence of protist communities shown by the variations in the Bray-Curtis dissimilarity index between samples collected along the 2009-2016 period, as a function of increasing lag between sampling dates. The lag values between samples, for each box plot correspond to a number of years (facet labels, from 0 to 7) plus a number of months (x axis of each facet, expressed as ranges). For example, the lag between samples considered for the first box plot is 0 years and 0 to 1 months and the lag between samples considered for the last box-plot in 7 years and 11 to 12 months. Panels **(A)** and **(C)** are based on the morphological dataset (cell counts) while graphs **(B)** and **(D)** are based on the metabarcoding dataset.

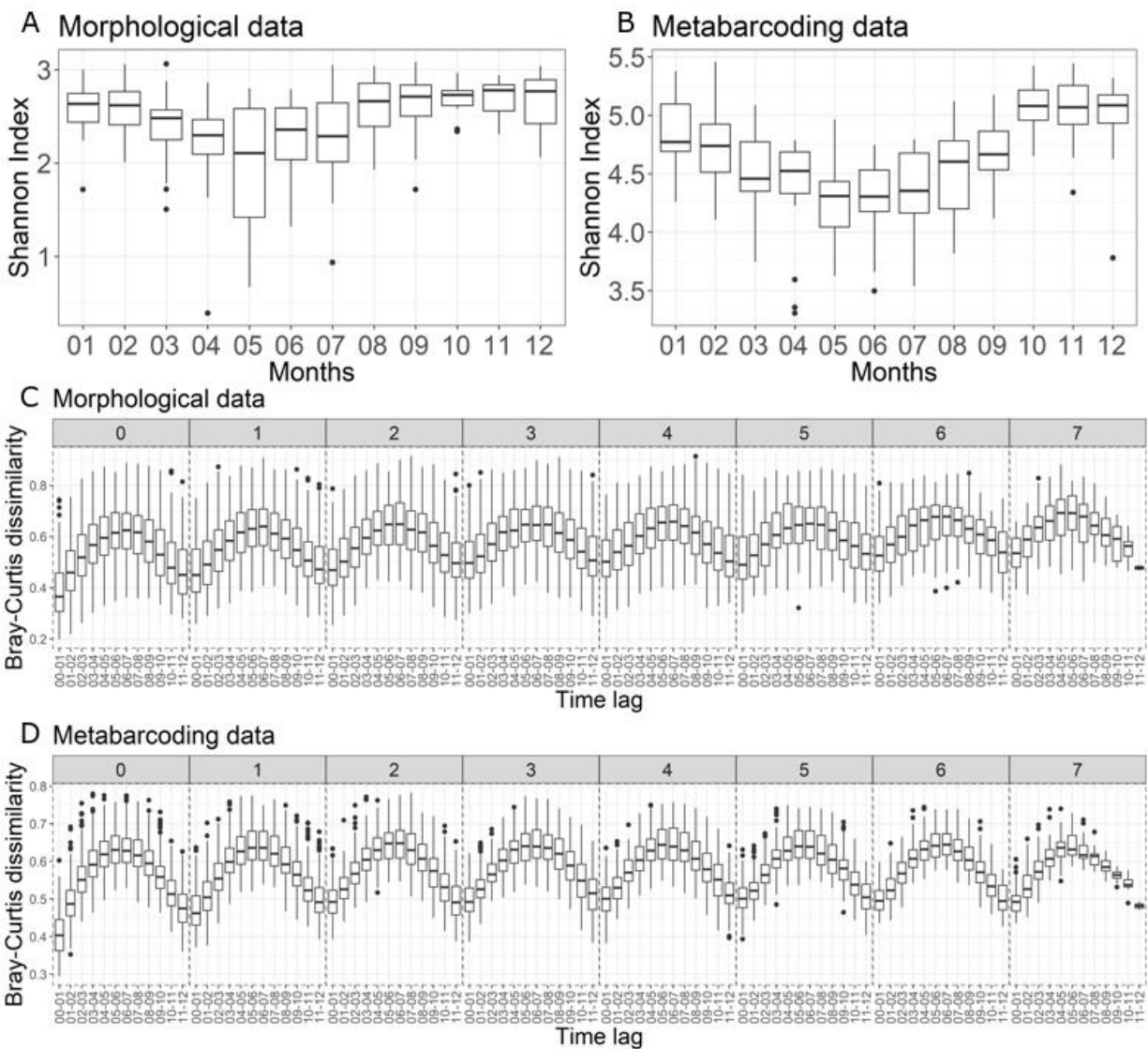


Figure 4

Low-taxonomic resolution contribution of protists at the SOMLIT-Astan time-series station over the period 2009-2016. Abundance of (A) the 12 main phytoplankton classes for the morphological dataset; and (B) the 52 main phyla - or classes – calculated from the metabarcoding dataset. The tree maps show the overall contributions of the main phyla or classes to the (C) total species or (D) OTU richnesses.

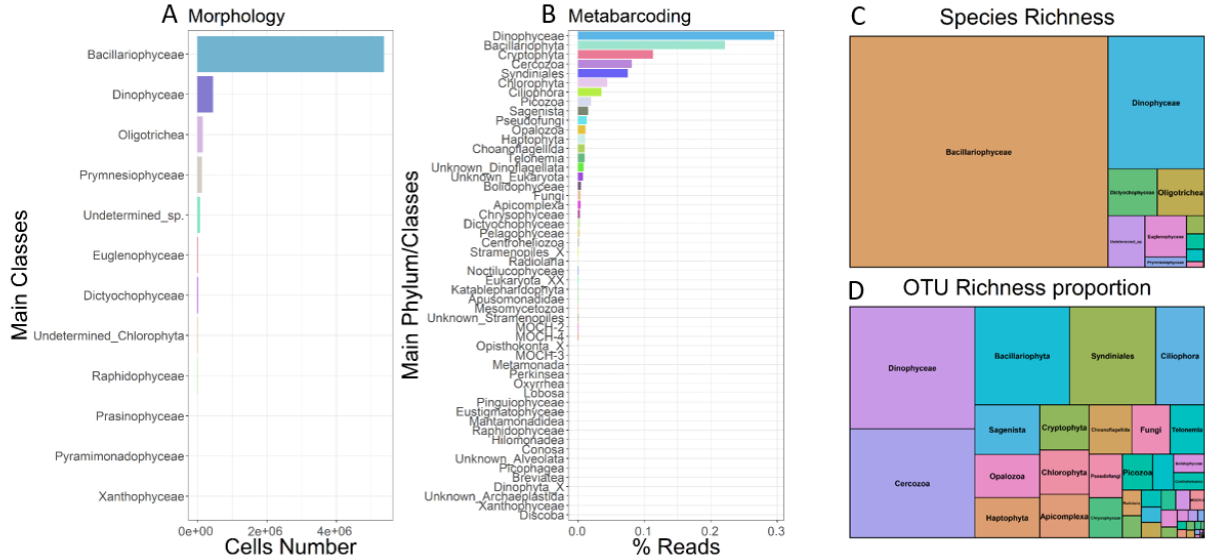


Figure 5

Typical seasonal variations of the dominant OTUs and overall contribution of the major diatoms species to the protist assemblage at the SOMLIT-Astan sampling station over the period 2009-2016. The histograms show the contributions (A) to total DNA reads abundance of the 32 dominating OTUs (accounting for 51.5% of all reads), (B) of the main diatoms to total diatoms abundances (microscopy count of plankton >10um) and (C) of the main diatoms to total diatom reads abundances. All microscopy counts and OTUs were assigned at the highest taxonomic level. Species selected were the 10 most abundant (5 for diatoms) for at least one month, taking into account mean monthly abundances.

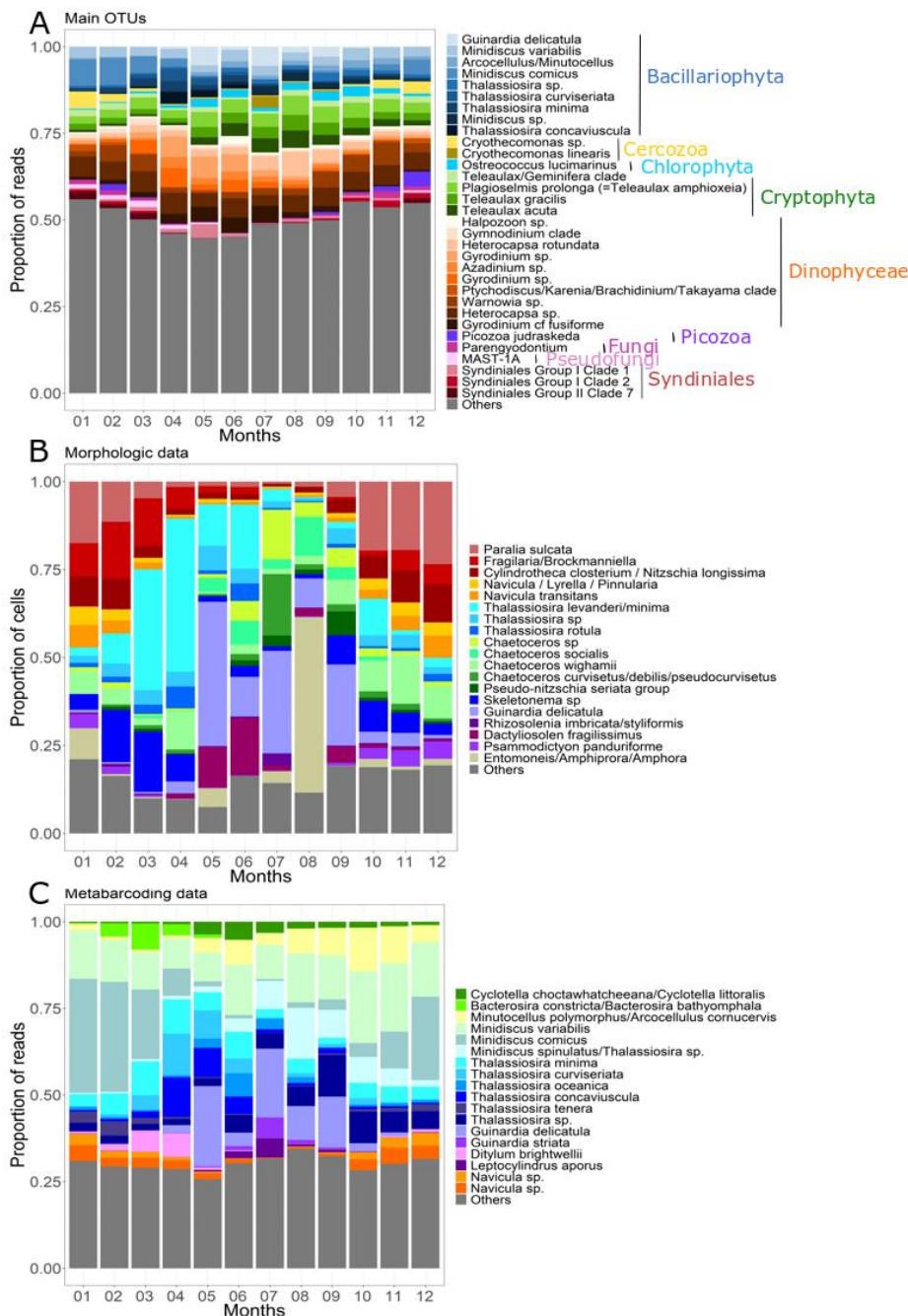


Figure 6

Similarity of protist communities (RDA analysis) in monthly samples over the period 2009-2016 at SOMLIT-Astan sampling station for morphological microscopy (A, B), and DNA metabarcoding (C, D) datasets. (A, C): Annual cycle of protist communities obtained by ordination of the monthly samples through a redundancy analysis (RDA) explaining (A) 48,9 % and (C) 52,2 % of the total variance of the community, respectively. (B, D): Decomposition of RDA axes that reveals seasonal pattern (RDA1; 19,8-17,8 % and RDA2; 11,5-9,3 %) and biannual broad scale oscillation (RDA3; 4,8-3,9 %).

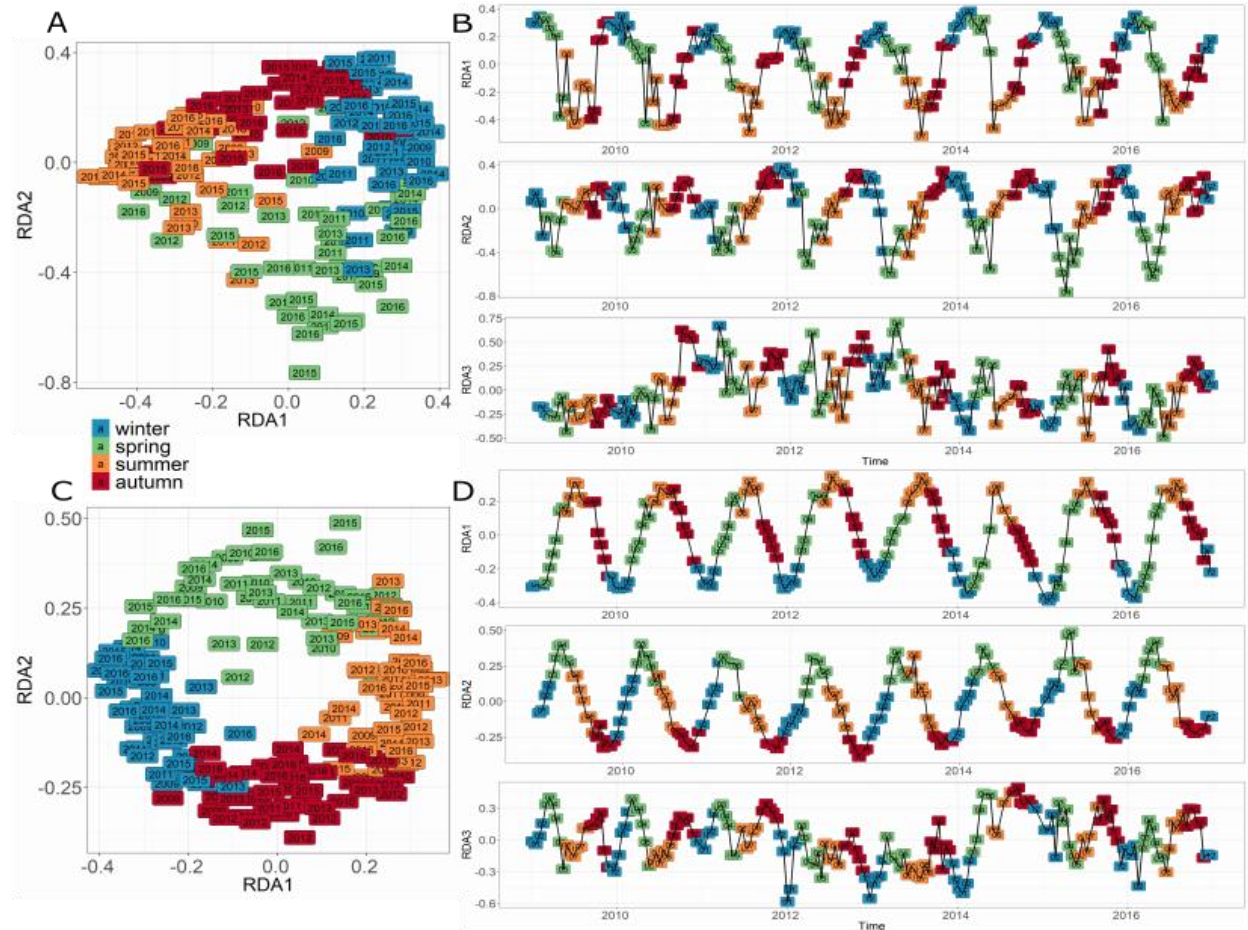


Figure 7

Monthly mean abundance (2009-2016), at the SOMLIT-Astan sampling site, for (A) the morphological species and (B) molecular OTUs as a function of the first three RDA axes (see Figure 6). For each RDA axis the (A) 10 species and (B) 10 OTUs with the highest score were selected. The * indicates dominant OTUs (reported in Fig.5).

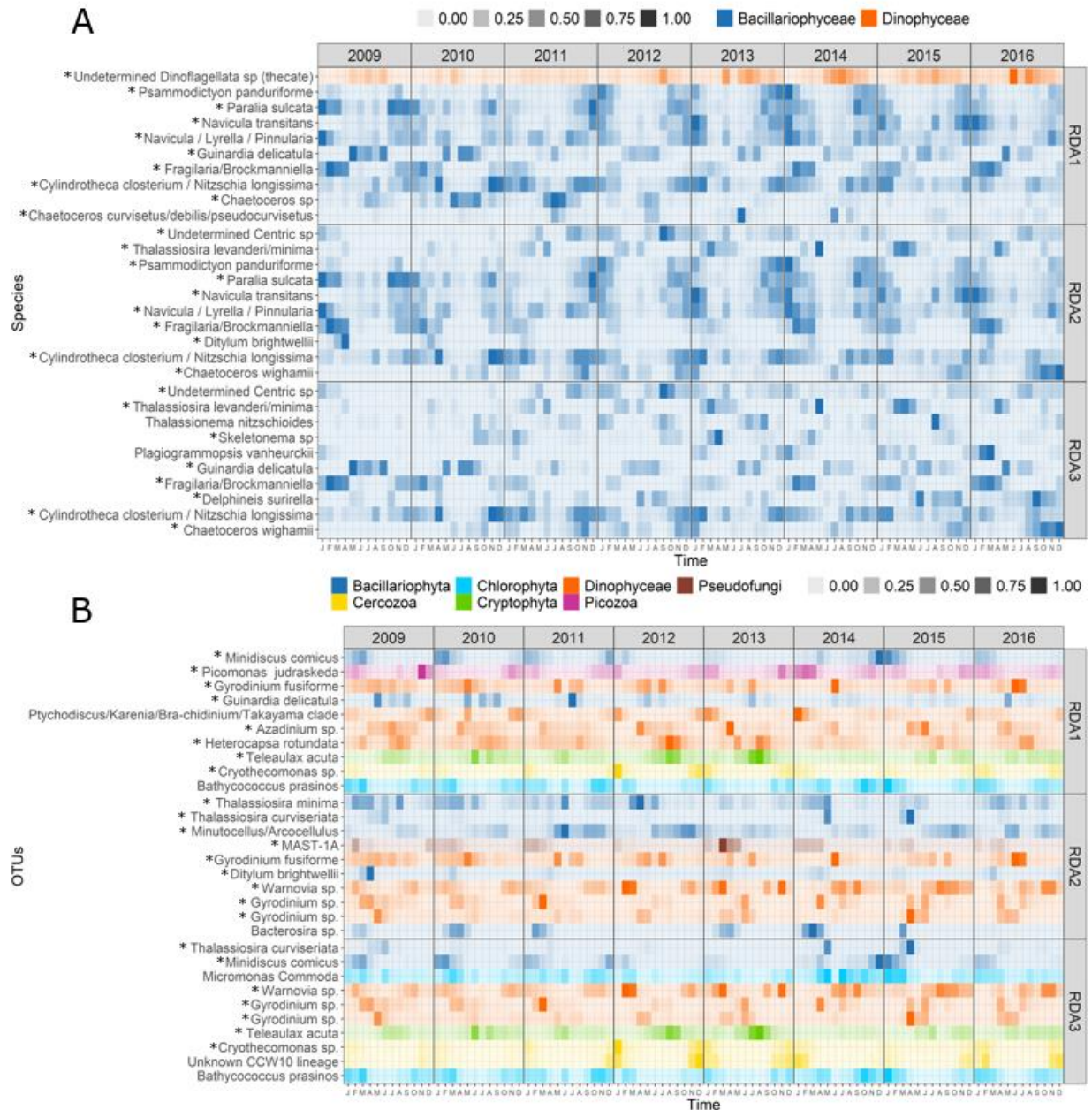


Figure 8

Spearman correlation calculated between the environmental variables and the RDA axes (A, C), and variance partitioning analyses between environmental drivers and dbMEM (B, D). Spearman correlations were computed between each axes of the RDA and each environmental parameter selected for (A) morphology and (B) metabarcoding. Variance partitioning between selected environmental variables and dbMEM was also calculated for (C) morphology and (D) metabarcoding data, respectively.

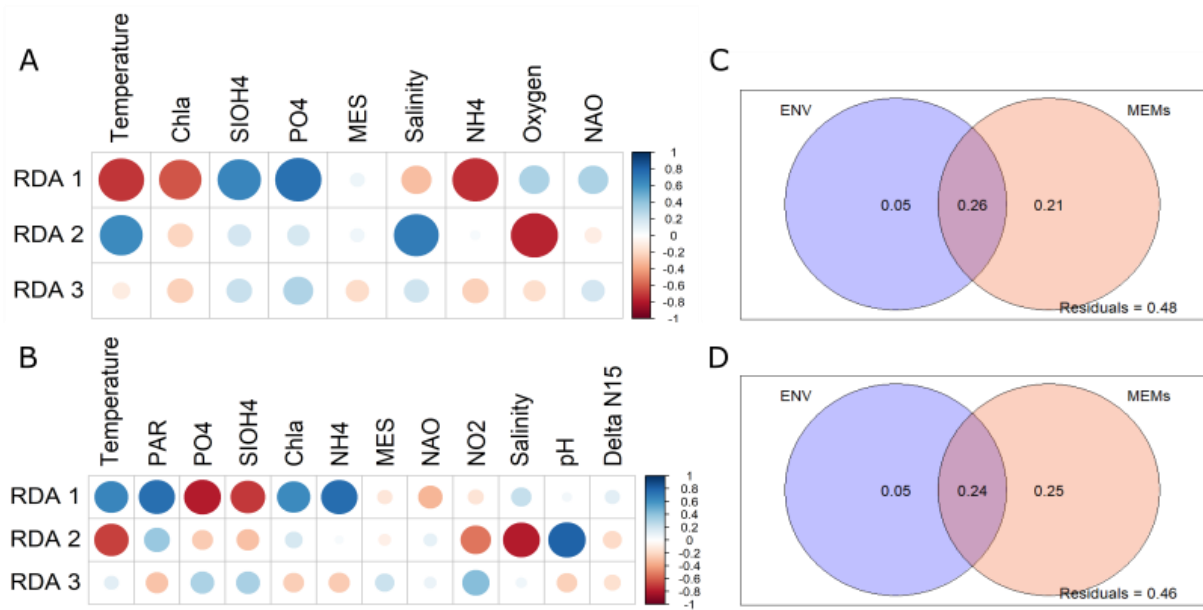


Table 1

Species and OTUs driving the seasonal oscillation showed in the RDA axes 1 and 2 and the biannual broad scale oscillations observed in axes 3. The 10 species/OTUs with the highest scores in each relative axes of the RDA were selected. The scores and the relative contributions to total abundance of the resulting list of species/OTUs are shown. For metabarcoding data, see Material and methods section and table S1 for assignments details.

| Species / Assignment | Contribution to variation axis 1 (%) | Contribution to variation axis 2 (%) | Contribution to variation axis 3 (%) | Contribution to total abundance (%) |
|--|---|---|---|--|
| Morphological dataset | | | | |
| <i>Chaetoceros curvisetus/debilis/pseudocurvisetus</i> | 2.4 | - | - | 1.3 |
| <i>Chaetoceros</i> sp. | 3.0 | - | - | 2.7 |
| <i>Chaetoceros wighamii</i> | | 3.7 | 18.3 | 3.0 |
| <i>Cylindrotheca closterium / Nitzschia longissima</i> | 3.9 | 2.0 | 2.0 | 5.9 |
| <i>Delphineis surirella</i> | - | - | 0.8 | 1.6 |
| <i>Ditylum brightwellii</i> | - | 1.6 | - | 0.5 |
| <i>Fragilaria/Brockmanniella</i> | 20.2 | 8.5 | 10.5 | 5.7 |
| <i>Guinardia delicatula</i> | 28.2 | - | 8.48 | 8.7 |
| <i>Navicula / Lyrella / Pinnularia</i> | 2.5 | 1.33 | - | 2.7 |
| <i>Navicula transitans</i> | 2.4 | 3.0 | - | 2.7 |
| <i>Paralia sulcata</i> | 12.5 | 15.7 | - | 10.6 |
| <i>Plagiogrammopsis vanheurckii</i> | - | - | 0.97 | 0.4 |
| <i>Psammodictyon panduriforme</i> | 1.9 | 4.69 | - | 1.8 |
| <i>Skeletonema</i> sp. | - | - | 43.2 | 4.0 |
| <i>Thalassiosira levanderi/minima</i> | - | 45.7 | 5.0 | 6.6 |
| <i>Thalassionema nitzschioides</i> | - | - | 0.91 | 0.7 |
| <i>Undetermined Centric</i> | - | 2.5 | 1.2 | 1.9 |
| <i>Undetermined Dinoflagellata (thecate)</i> | 2.9 | - | - | 6.2 |
| Metabarcoding dataset | | | | |
| <i>Bacterosira</i> sp. | - | 1.9 | - | 0.3 |
| <i>Bathycoccus prosinos</i> | 1.5 | - | 1.86 | 0.9 |
| Unknown CCW10 lineage | - | - | 2.3 | 0.3 |
| <i>Cryothecomons</i> sp. | 3.2 | - | 6.4 | 1.4 |
| <i>Teleaulax acuta</i> | 2.4 | - | 2.2 | 2.2 |
| <i>Heterocapsa rotundata</i> | 2.1 | - | - | 2.4 |
| <i>Gyrodinium</i> sp. | - | 5.7 | 2.9 | 2.2 |
| <i>Azadinium</i> sp. | 2.2 | - | - | 1.1 |

| | | | | |
|---|------|-----|-----|-----|
| <i>Gyrodinium</i> sp. | - | 7.1 | 2.5 | 1.7 |
| <i>Ptychodiscus/Karenia/brachydinium/takayama clade</i> | 1.4 | - | - | 0.5 |
| <i>Warnovia</i> sp. | - | 2.2 | 7.6 | 3.2 |
| <i>Ditylum brightwellii</i> | - | 2.2 | - | 0.4 |
| <i>Guinardia delicatula</i> | 4.1 | - | - | 1.5 |
| <i>Gyrodinium cf fusiforme</i> | 1.8 | 2.2 | - | 2.1 |
| MAST-1A | - | 2.3 | - | 0.5 |
| <i>Micromonas commoda</i> | - | - | 1.9 | 0.8 |
| <i>Picomonas judraskeda</i> | 1.5 | - | - | 0.7 |
| <i>Minidiscus comicus</i> | 10.0 | - | 6.1 | 2.7 |
| <i>Minutocellus/Arcocellulus</i> | - | 2.2 | - | 1.0 |
| <i>Thalassisira minima</i> | - | 2.0 | - | 1.2 |
| <i>Thalassisira curviseriata</i> | - | 3.0 | 2.7 | 0.7 |